EUROPEAN COMMISSION

European Research Area

CArbon-14 Source Term

CAST

Development of a Compound-specific Carbon-14 AMS Technique for the Detection of Carbon-14 Labelled Organic Compounds (D2.3)

E. Wieland, B. Cvetković

Date of issue of this report: 25/1/2016

The project has received funding from the European Union's European Atomic Energy Community's (Euratom) Seventh Framework Programme FP7/2007-2013 under grant agreement no. 604779, the CAST project.		
Dissemination Level		
PU	Public	**X**
RE	Restricted to the partners of the CAST project	
CO	Confidential, only for specific distribution list defined on this document	

EURATOM

EUROPEAN
COMMISSION

European
Research Area

CAST – Project Overview

The CAST project (CArbon-14 Source Term) aims to develop understanding of the potential release mechanisms of carbon-14 from radioactive waste materials under conditions relevant to waste packaging and disposal to underground geological disposal facilities. The project focuses on the release of carbon-14 as dissolved and gaseous species from irradiated metals (steels, Zircaloys), irradiated graphite and from ion-exchange materials.

The CAST consortium brings together 33 partners with a range of skills and competencies in the management of radioactive wastes containing carbon-14, geological disposal research, safety case development and experimental work on gas generation. The consortium consists of national waste management organisations, research institutes, universities and commercial organisations.

The objectives of the CAST project are to gain new scientific understanding of the rate of release of carbon-14 from the corrosion of irradiated steels and Zircaloys and from the leaching of ion-exchange resins and irradiated graphites under geological disposal conditions, its speciation and how these relate to carbon-14 inventory and aqueous conditions. These results will be evaluated in the context of national safety assessments and disseminated to interested stakeholders. The new understanding should be of relevance to national safety assessment stakeholders and will also provide an opportunity for training for early career researchers.

For more information, please visit the CAST website at:
http://www.projectcast.eu

CAST		
Work Package: 2	CAST Document no. :	Document type:
Task: D2.3	CAST-2015-D2.3	R
Issued by: PSI		Document status:
Internal no. : CAST_Report_D.2.3		Final

Document title
Development of a compound-specific carbon-14 AMS technique for the detection of carbon-14 labelled organic compounds

Executive Summary

Carbon-14 is an important radionuclide in the inventory of radioactive waste and is considered to be a key radionuclide in performance assessment. For example, the ^{14}C inventory in the planned cement-based repository for low- and intermediate-level radioactive waste in Switzerland is mainly associated with activated steel (~85 %). Therefore, anoxic corrosion of the activated steel will determine the time-dependent release of ^{14}C bearing compounds from the cementitious near field into the host rock.

The current situation concerning the carbon species generated in the course of the anoxic corrosion of iron/steel (activated/irradiated and non-activated/irradiated) is still unclear. Neither experimental evidence nor thermodynamic modelling allows well-supported conclusions to be drawn regarding the kind of organic compounds formed. The currently unclear situation requires further experimental investigations into the formation of organic compounds during the anoxic corrosion of activated and non-activated iron/steel in conditions relevant to a cement-based repository.

This report outlines the design of an experiment to determine the speciation of ^{14}C released during the anoxic corrosion of activated steel under the relevant repository conditions. The project was launched and is being carried out in the framework of the Swiss waste management programme and co-financed by the EU project “CAST”. This report summarizes the results from the first phase of the project.

List of Contents

1 Introduction

Carbon-14 has been identified as a radionuclide of importance in the inventory of radioactive waste produced in many European countries as well as a key radionuclide in radiological assessments [Johnson and Schwyn, 2008; Yim and Carron, 2006; Nagra, 2002; Nuclear Decommissioning Authority, 2012]. The half-life of ^{14}C is sufficiently long (5730 y) for its release to be of relevance after repository closure. Carbon-14 may be released from waste into solution or into the gas phase as inorganic or organic/hydrocarbon species, respectively. Carbon-14 is of specific concern because of its potential presence as either dissolved or gaseous organic species in the disposal facility and the host rock, the high mobility of dissolved organic compounds in the geosphere caused by weak sorption onto minerals under near neutral conditions, and eventually because ^{14}C in organic form can be incorporated in the human food chain. Hence, the forms of ^{14}C bearing species define the routes of release to be considered in safety assessments of ^{14}C migration from the engineered system of a geological repository.

In nuclear power plants ^{14}C is produced in the fuel, from core structural materials, and in reactor coolant due to the interaction of thermal neutrons with the (stable) parent isotopes ^{14}N, ^{17}O and ^{13}C [Yim and Caron, 2006]. In light water reactors (LWR) the formation of ^{14}C is primarily caused by nitrogen impurities contained in nuclear fuel and metal components of the core structural materials by ^{14}N activation (^{14}N (n,p) ^{14}C). The production from carbon impurities and oxygen in metals, however, is negligible as the ^{13}C and ^{17}O contents are low. In addition, the capture cross-section of ^{13}C for thermal neutrons is very low. Transmutation of ^{17}O in water molecules ($^{17}O(n,\alpha)^{14}C$), transmutation of nitrogen dissolved in water by $^{14}N(n,p)$ ^{14}C and ^{13}C (present as bicarbonate and organic compounds) by $^{13}C(n,\gamma)$ ^{14}C in reactor coolant are other possible sources of ^{14}C in low- and intermediate-level waste (L/ILW). In Switzerland the main source of ^{14}C in L/ILW are activated metallic nuclear fuel components and reactor core components as well as spent filters and ion exchange resins used in the LWRs for the removal of radioactive contaminants in a number of liquid processes and waste streams. Compilation of the activity inventories reveals that in the already existing and future arising of radioactive waste in Switzerland, the ^{14}C inventory is

mainly associated with activated steel (~ 85 %) while the ^{14}C portions from nuclear fuel components (e.g. Zircaloy) and waste from the treatment of reactor coolants are much smaller.

Upon release from the activated steel parts ^{14}C can exist in the inorganic chemical form (e.g. CO, CO_2, HCO_3^- and CO_3^{2-}) or organic chemical form in solution or gas phase depending on the nature of the waste material and the chemical conditions of the near field. In the inorganic form ^{14}C will decay within a disposal facility as $^{14}CO_2$ (and its bases) is strongly retarded in the cementitious near field by precipitation as calcium carbonate or isotopic exchange with stable CO_3^{2-} in calcium carbonate [Allard *et al.*, 1981; Bayliss *et al.*, 1988; Pointeau *et al.*, 2003]. Therefore, inorganic ^{14}C has only a negligible effect on dose release. In contrast, dissolved and gaseous species containing ^{14}C are only very weakly retarded by cementitious materials.

Low molecular-weight (LMW) oxygenated ^{14}C bearing organic compounds, e.g. acetate, formate, acetaldehyde, formaldehyde, methanol, and ethanol were found to form in the course of steel corrosion (see Section 2; see review by [Swanton *et al.*, 2014]). Studies on the uptake of these compounds by mortar indicate weak interaction with cementitious materials [Matsumoto *et al.*, 1995; Noshita *et al.*, 1996; Sasoh, 2008a; Wieland and Hummel, 2015]. This implies that ^{14}C mainly contributes to dose release due to migration in its organic form in solution, such as ^{14}C bearing LMW organics, or as gaseous species.

Information on the chemical form of carbon released during corrosion of irradiated metals, such as Zircaloy and irradiated steel, is limited (see review by [Swanton *et al.*, 2014]). Studies with irradiated and non-irradiated stainless steel were conducted in the framework of the Japanese disposal programme for radioactive waste by [Yamaguchi *et al.*, 1999; Kaneko *et al.*, 2003; Sasoh, 2008 b/c; Noshita, 2008; Kani *et al.*, 2008; Yamashita *et al.*, 2014; Takahashi *et al.*, 2014]. Additional information is available from corrosion studies with non-irradiated iron powders carried out in connection with the development of clean-up techniques for chlorinated hydrocarbons using zero-valent iron [Hardy and Gillham, 1996; Campbell *et al.*,1997; Deng *et al.*,1999; Agrawal *et al.*, 2002]. In these studies both oxidized and reduced hydrocarbons have been observed in iron-water systems in anoxic

near neutral to alkaline conditions. The formation of reduced hydrocarbons, such as methane and other volatile compounds, is expected due to the reducing conditions that prevail at the iron-water interface and as a result of the hydrolysis of carbide species in the iron (see review by [Swanton *et al.*, 2014]). The formation of oxidized hydrocarbons, however, appears to be inconsistent with the negative redox potential at the iron-water interface. Note that all studies reported the formation of only organic compounds with a low molecular weight and with a low number of carbon atoms ($C \leq 5$).

The current situation concerning the carbon speciation in the course of the anoxic corrosion of iron/steel (activated/irradiated and non-activated/irradiated) is thus not well understood. In particular, it is unclear why both reduced and oxidized hydrocarbons may exist simultaneously in solutions in contact with corroding iron and steel. In principle, predominant formation of reduced hydrocarbons is expected, such as the formation of volatile alkanes and alkenes, in view of the strongly reducing conditions prevailing at the iron-water interface in alkaline solution. Nevertheless, there is enough experimental evidence indicating that also oxidized species exist in alkaline iron-water systems. Presence of oxidized species is conceivable in systems containing irradiated materials due to radiolysis while residual oxygen at the iron-water interface could act as an oxidizing agent in non-irradiated systems. At present, the reason for the existence of oxidized species and the chemical conditions and reactions leading to these compounds is not yet understood. The predominance of organic compounds was further assessed with the help of thermodynamic modelling [Wieland and Hummel, 2015]. The authors concluded that the predictive capability of thermodynamic modelling is limited due to uncertainties associated with the concept of meta-stability in the C-H-O system.

The currently unclear situation concerning the carbon speciation in anoxic alkaline conditions requires further experimental investigations into the formation of organic compounds during the anaerobic corrosion of activated and non-activated iron and steel, and, in addition, into the chemical stability of organic compounds in conditions relevant to a cement-based repository.

2 PSI Research on Carbon-14 Bearing Compounds

The experimental programme launched at PSI aims at determining the ^{14}C containing species generated in the course of the anoxic corrosion of activated steel in alkaline solution. These conditions correspond to the geochemical conditions prevailing in a deep geological repository with a cementitious near field. The objective is further to investigate the corrosion behaviour of "real" samples, i.e. activated steel from a nuclear power plant.

2.1 *Lay-out of the Experimental Set-up*

A schematic view of the layout of the experimental set-up is displayed in Figure 1. The corrosion experiment will be carried out in a gas-tight autoclave-type reactor assembled behind a lead shielding. Off-line separation of compounds in the liquid and gas phases is followed by oxidation of the compounds to prepare samples for ^{14}C measurements using accelerator mass spectrometry (AMS).

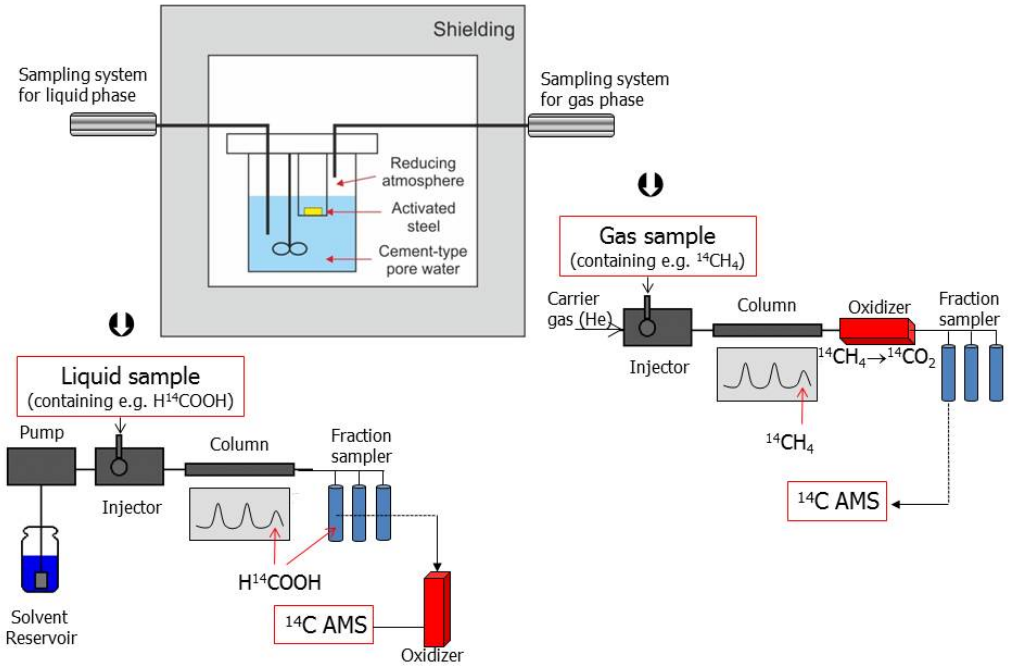

Figure 1: Schematic sketch of the set-up and analytical strategy for the planned corrosion experiment with activated steel at PSI.

The solution should have an ionic composition similar to that of the pore solution of the cementitious environment. Selected parameters will be monitored (temperature, oxygen, pressure) with the aim of controlling the physico-chemical conditions inside the reactor. Careful control of sample manipulations is required, such as sampling of liquid and gaseous phase, to minimize/avoid ingress of oxygen into the reactor. The compound-specific ^{14}C AMS method is developed as an off-line technique to identify and quantify the ^{14}C labelled gaseous and dissolved compounds.

The research plan for the corrosion experiment with activated steel was developed in view of the experimental and analytical constraints that are outlined in the following section.

2.2 *Experimental Constraints*

2.2.1 Amount of Activated Steel

The amount of activated steel that was obtained from the nuclear power plant Gösgen in Switzerland (NPP Gösgen) was limited to avoid significant extra costs. In the course of the annual maintenance work in NPP Gösgen five guide-tube nuts (~ 5 g each) had been retrieved from the storage pool and transferred to the hot laboratory of PSI in 2012. The nuts made of stainless steel had been mounted at the top and bottom end of fuel rods and subjected to irradiation in the nuclear reactor core of NPP Gösgen for two years. The activation cycle was terminated in June 2011. Each nut has a contact dose rate of ~ 150 mSv/h. Two nuts were processed in the PSI hot laboratory to prepare small specimens for laboratory experiments [Schumann *et al.*, 2014].

2.2.2 Sample Size

The amount of activated steel used in the planned corrosion experiment is largely determined by the regulations of radiation protection that require an effective lead shielding in order to minimize exposure. Thus, at the given high dose rate of the steel nuts from NPP Gösgen an appropriate lead shielding has to be installed. The high dose rate is caused by the large inventories of ^{60}Co and ^{54}Mn in activated steel. In the process of evaluating possible options for shielding it emerged that the hot cell in the PSI hot laboratory available for

emplacing the corrosion reactor is not suitable because of its limited inside space. It was not possible to ensure proper handling during operation of the reactor such as liquid and gas sampling. Therefore, it was decided to assemble the reactor behind a conventional lead shielding with a wall thickness of 5 cm. As a consequence, the sample size had to be reduced in a way that the dose rate in the vicinity of the reactor will reach a level in accordance with the regulations and also complied with the rules of the PSI hot laboratory. Dose calculations showed that a maximum of 5 g activated steel (i.e. one steel nut at most) can be emplaced in the shielded corrosion reactor.

2.2.3 Carbon-14 Content of Activated Steel

The ^{14}C content in the irradiated stainless steel nuts from the NPP Gösgen was determined experimentally using a wet chemistry digestion technique combined with liquid scintillation counting for ^{14}C activity measurements. Details of the experimental method and a comparison with theoretical predictions of the ^{14}C content made on the basis of a Monte Carlo reactor model for NPP Gösgen have been reported by [Schumann *et al.*, 2014]. The ^{14}C activity was determined experimentally to be ~ 17800 Bq in 1 g steel nut, which corresponds to a ^{14}C content of only 0.107 µg g^{-1} (0.107 ppm).

2.2.4 Corrosion Rate

Iron and steel are in a passive state in alkaline solutions, such as cement pore water, under fully anoxic conditions and therefore, corrosion rates are expected to be extremely low. Formation of the corrosion products $Fe(OH)_2$ and, as a result of the Schikorr reaction, Fe_3O_4 occurs, thereby forming a passive layer on iron-based alloys. Thus, passivation occurs due to the formation of a non-porous oxide film with a thickness of a few nanometres, similar to that under near neutral conditions. Reviews of corrosion rates in anoxic alkaline conditions have been reported elsewhere [Smart *et al.*, 2004; Diomidis, 2014; Swanton *et al.*, 2014].

Corrosion studies indicate that stainless and carbon steel surfaces are able to form a passivating layer under anoxic alkaline conditions by direct reaction with water. Austenitic and ferritic alloys (e.g. stainless steel) tend to corrode slower than carbon steel in these conditions due to the presence of the alloying elements chromium, nickel or molybdenum,

respectively. Corrosion rates for carbon steel were found to range in value between 0.1 and 1 µm a^{-1} under anoxic alkaline conditions [Smart *et al.*, 2004]. Even lower corrosion rates have been reported for stainless steel and Zircaloy (typically < 0.01 µm a^{-1}, range: 0.001 µm a^{-1} - 0.02 µm a^{-1}; [Diomidis, 2014; Swanton *et al.*, 2014]).

2.2.5 Expected Carbon-14 Concentrations

The low corrosion rate in combination with the relatively low ^{14}C content in the stainless steel nuts and the small amount of material that can be used result in an extremely low amount of ^{14}C released during the planned corrosion experiment. Scoping calculations were carried out with the aim of estimating the aqueous concentration of ^{14}C for a typical set-up: 1 g stainless steel nut (surface area: 1.5 cm^2 g^{-1}; ^{14}C content: 0.107 µg g^{-1}; linear corrosion rate: 0.001 µm a^{-1}) in contact with 300 mL alkaline solution (gas phase: 200 mL). The total amount of ^{14}C produced is estimated at ~ $3 \cdot 10^{-17}$ mol d^{-1} (~ $7 \cdot 10^{-5}$ Bq d^{-1}), which corresponds to an aqueous ^{14}C concentration of ~10^{-16} mol L^{-1} d^{-1} (~ $2 \cdot 10^{-4}$ Bq L^{-1} d^{-1}), if no ^{14}C bearing gaseous species are formed. It is further estimated that the ^{14}C content in the samples used for the ^{14}C measurements with AMS amounts to < 10^{-18} mol d^{-1} (~ $2 \cdot 10^{-6}$ Bq d^{-1}) on the assumption that only 10 mL aliquots at maximum can be sampled from the liquid phase and that several ^{14}C bearing compounds exist. It should be noted that the ^{14}C concentration in the samples will increase with time, i.e. it will be a factor of 100 higher after 100 days corrosion. In any case, the ^{14}C concentration in the samples is expected to range between ~ 10^{-16} mol L^{-1} after 1 day (~ $2 \cdot 10^{-4}$ Bq L^{-1}) and ~10^{-14} mol L^{-1} after 100 days (~ $2 \cdot 10^{-2}$ Bq L^{-1}) during the corrosion experiment with activated steel.

2.3 *Analytical Constraints*

The aim of this project is to identify the ^{14}C bearing compounds that are produced in the course of the anoxic corrosion of activated steel, which requires development of single compound analysis. To this end, specific analytical separation techniques and the development of compound-specific analytical methods both for the aqueous and gaseous species are needed which will allow extremely low ^{14}C concentrations to be detected.

Hence, chromatographic separation techniques have to be coupled to a very sensitive detection method for ^{14}C, such as ^{14}C AMS.

2.3.1 Chromatographic Separation Techniques

Gas chromatography (GC) is the classical technique used to separate and, in combination with a mass spectrometer, to identify single volatile compounds. The small molecules expected to form in this study can be separated with the help of suitable columns. The equipment and methods used at PSI are reported in Section 3.2. Oxidation of the single compounds generates $^{14}CO_2$ which is collected as separate fractions in conjunction with ^{14}C quantification using the AMS (Figure 1). To this end, a fraction sampling system is currently being developed at PSI.

Dissolved organic compounds can be separated using either high performance liquid chromatography (HPLC) [Takahashi *et al.*, 2014] or ion chromatography (IC) [Chi and Huddersman, 2007]. The equipment and methods used at PSI are reported in Section 3.1. After IC separation the single compounds are collected in separate fractions. Small aliquots of the liquid phase are oxidized to generate $^{14}CO_2$ which is directly injected into the ^{14}C AMS (Figure 1).

2.3.2 Detection of Single Compounds

The limit of detection (LOD) for dissolved organic compounds using classical IC separation with a conductivity detector (CD) or mass spectrometer (MS), respectively, is typically on the ppb level. The limit is determined by the class of compounds to be separated and the matrix in which the species have to be separated. For example, the detection limit of a high performance ion exclusion chromatography (HPIEC) system currently in operation in PSI, which was used for the analysis of short-chain aliphatic carboxylic acids in alkaline media, was found to be 0.1 µM organic acid, i.e. ~ 6 ppb [Glaus *et al.*, 1999]. The equipment used by the authors consisted of a DX-600 chromatograph (Dionex, Switzerland) equipped with a 9x250 mm IonPac ICE-AS6® column (Dionex, Switzerland) and a CD combined with an AMMS-ICE anion exclusion micro-membrane suppressor.

The limit of detection (LOD) for volatile organic compounds using GC with flame ionization detection (FID) is on the sub-ppb to ppb level while a detection limit on the ppt to ppb level is achieved with MS detection. Pre-concentration of single compounds is a possible route to reach concentrations for measurements above the detection limit.

Liquid scintillation (LSC) is the standard method used to determine the ^{14}C activity. The detection limit for ^{14}C measurements using a conventional LSC is ~ 1 Bq L^{-1}. The limit may be a factor of ~100 lower if low level counting and specific radioanalytical procedures are employed (e.g. the benzene synthesis method, CO_2 absorption method). Thus, ^{14}C concentrations on the ppt level (parts-per-trillion, 10^{-12}) can be determined using radioanalytical methods.

The expected concentrations of the ^{14}C bearing organic compounds in the planned corrosion experiment with activated steel using the available experimental set-up is estimated to be on the sub ppq level (parts-per-quadrillon, 10^{-15}) (Section 2.2.5). The required sensitivity of the analytical method for a compound-specific characterization of the gas and liquid phase is thus expected to be several orders of magnitude lower than the detection limits provided by classical detection systems such as MS. Furthermore, it is also lower than ^{14}C activity measurements with LSC for liquid phase analysis. Therefore, extremely efficient pre-concentration of the compounds of interest would be needed to allow the identification of single compounds using the aforementioned classical detection systems. Artefact-free pre-concentration is a major challenge, in particular for volatile hydrocarbons with the number of carbon atoms ≤ 5, e.g. methane, ethane, etc.

An analytical route based on compound-specific ^{14}C AMS detection is taken into consideration in conjunction with the planned corrosion experiment with activated steel. The main reason is that ^{14}C AMS is an extremely sensitive ^{14}C detector (limit of detection (LOD): 10^{-18} g ^{14}C). In combination with chromatographic separation, this should allow ^{14}C bearing compounds to be determined at extremely low concentrations. As previously outlined these low ^{14}C concentrations are caused by the experimental constraints: the very low corrosion rate, the small amount of activated steel that can be used, the low ^{14}C

inventory of activated steel, small volumes of the gas and liquid samples that have to be withdrawn from the reactor, and sample dilution during the chromatographic separation process (dilution with eluent or carrier gas, partition into different ^{14}C containing single compounds).

2.4 Experimental and Analytical Strategy

Due to the particular requirement, the development of the set-up and analytical techniques for the planned corrosion experiments with activated steel was divided into several tasks:

1) Determination of the ^{14}C concentration in the activated steel nuts;
2) Development of a reactor system for the corrosion experiment with activated steel;
3) Development of analytical methods for the separation of gaseous and dissolved organic compounds using ion and gas chromatography;
4) Identification of the carbon species (dissolved, gaseous) generated during the anoxic corrosion of non-activated iron powders;
5) Development of the compound-specific ^{14}C AMS-based analytical methods for the identification and quantification of the compounds identified in task 4.

The results obtained in tasks 1 and 2 are not summarized in this report as they are not part of PSI's contribution to CAST. Task 1 is finished and the results have been published elsewhere [Schumann *et al.*, 2014]. The following sections describe the state of research at PSI in connection with tasks 3 - 5.

3 Development of Analytical Methods

Developments of the HPIEC-MS and GC-MS analytical methods undertaken in relation to task 3 are aimed at separating, identifying and quantifying the aqueous and gaseous carbon compounds formed during the corrosion of iron/steel. The developments comprise analysis of carboxylates, headspace analysis of hydrocarbons as well as alcohols and aldehydes from aqueous media, and the analysis of hydrocarbons in the gas phase analysis.

3.1 *High Performance Ion Exclusion Chromatography (HPIEC)*

An ICS-5000 ion chromatography system (Dionex/Thermo Fisher, Sunnyvale, CA, USA) consisting of an EG 40 eluent generator, an AS 50 auto sampler, a CD 25 conductivity detector (Dionex/ Thermo Fisher, Sunnyvale, CA, USA), and a coupled MSQ™ Plus (Thermo Fisher, Sunnyvale, CA, USA) mass spectrometer (MS) with an atmospheric pressure ionization (API) interface, operated in the negative electrospray ionization (ESI) mode was used for HPIEC. The carboxylic acids were separated using a 250 mm × 2 mm i.d. IonPac AS11-HC column in combination with the corresponding guard column (Dionex/Thermo Fisher, Sunnyvale, CA, USA). A 2 mm AERS–500 suppressor (Dionex/ Thermo Fisher, Sunnyvale, CA, USA) operated in the external water mode was placed before the conductivity cell. The analytical column was operated at 30°C (column thermostat TCC-100, Dionex/Thermo Fisher, Sunnyvale, CA, USA). During this time period the KOH mobile phase was discarded via a separate outlet. The optimized mobile phase consisted of KOH, produced by the eluent generator with the following gradient scheme: KOH: 0-15 min: isocratic with 1.0 mM; 15-35 min: gradient from 1 → 30 mM; 35-40 min: isocratic with 30 mM; 40-41 min: gradient from 30 → 1 mM; 41-46 min: isocratic 1 mM. 10 µL of the samples were injected via a 10 µL loop and eluted using a flow rate of 0.25 mL min^{-1}. The HPIEC separation of the dissolved LMW organics was optimized with respect to column type, mobile phase, and gradient dynamics to achieve the greatest possible selectivity and sensitivity. The IonPac AS11-HC column was used because well-resolved peak shapes were obtained for all analytes.

The ESI probe temperature was 500 °C, cone voltages varied from 30 to 50 V, and ESI needle voltage was -3.0 kV. High-purity N_2 (99.99995 %, Messer Schweiz AG, Lenzburg, Switzerland), supplied by a separate nitrogen tank, served as protecting and nebulizing gas, maintaining a nitrogen pressure of 80 psi. The following parameters were used for MS detections: RF-lens: −1.0 V; mass span: 0.5 u; dwell-time: 0.25 s. The analytes were monitored in the selected ion monitoring (SIM) mode observing the m/z values of the compounds of interest using five different time slots. Signal areas (counts min^{-1}) were used as quantitative measure. In addition, negative ion full scan mass spectra were recorded over the m/z range of 1–300 at a scan time of 0.5 s.

Data acquisition, processing and system control of the IC were accomplished with the Chromeleon 6.80 (SR11d) software, while the Xcalibur Finnigan Surveyor MSQ 1.1 ELMO was the MS control software.

Chemical reagents used for HPIEC included: sodium acetate (puriss. p.a., Sigma Aldrich GmbH, Buchs, Switzerland), sodium formate (puriss. p.a., Sigma Aldrich GmbH, Buchs, Switzerland), malonic acid (reagent grade 99.5 %, Alfa Aeser, Karlsruhe, Germany), and oxalic acid (anhydrous for synthesis, Merck Schuchardt OHG, Hohenbrunn, Germany). The isotopic labelled internal standards (ILIS) (d-formic acid, acetic acid-2,2,2-d_3, 1,3-$^{13}C_2$-malonic acid, oxalic acid-$^{13}C_2$ dihydrate, and valeric-d_9 acid purity grade for all labelled compounds > 99.5 %) were obtained from Sigma Aldrich (Buchs, Switzerland).

Crystalline compounds from sodium acetate, sodium formate, malonic acid, and oxalic acid, respectively, were dissolved in 50 mL ultra-pure water to obtain individual stock solutions with concentrations of 10 mM. A multi-component stock solution (10 mL) containing sodium acetate, sodium formate, malonic acid, oxalic acid, and valeric acid with concentrations of 600, 200, 50, 50, and 100 µM, respectively, was prepared by diluting the individual stock solution with ultra-pure water. Aqueous calibration standards for the HPIEC measurements with sodium acetate, sodium formate, malonic acid, oxalic acid, and valeric acid in the concentration range 30-600, 10-200, 2.5-50, 2.5-50, and 5-100 µM, respectively, and the five respective ILIS with concentrations 300, 100, 25, 25, and 50 µM were prepared for each calibration in ultra-pure water using the multi-component stock

solution. All solutions were stored at 4 °C in the refrigerator. The analytical parameters are summarized in Table 1.

Table 1: Analytical parameters for quantification of the dissolved LMW organic compounds.

Compound	Retention Time R_f [min]	m/z	Cone Voltage [V]
Acetic acid	11.4	59	60
Acetic acid-2,2,2-d_3	11.5	62	60
Formic acid	14.3	45	60
Formic d-acid	14.1	46	60
Malonic acid	31.8	103	30
1,3-$^{13}C_2$-Malonic acid	31.8	105	30
Oxalic acid	34.6	89	30
Oxalic acid-$^{13}C_2$ dihydrate	34.6	91	30
Valeric acid	21.7	101	30
Valeric-d_9 acid	21.3	110	30

3.2 *Gas Chromatography (GC)*

A GC-MS system consisting of a 6890 gas chromatograph (Agilent Technologies, Waldbronn, Germany) and a 5973 mass spectrometer (Agilent Technologies, Waldbronn, Germany) with electron ionization (EI) was used. The equipment was operated with the MSD ChemStation D.03.00.611 software for data acquisition and processing.

3.2.1 Headspace Analysis of Hydrocarbons

Headspace analysis was performed using a Gerstel MSP2 multi-purpose sampler (Gerstel AG, Sursee). Headspace samples (2.5 mL) were injected after 30 min incubation at 50 °C under agitation using a heated (85 °C) syringe. The gaseous hydrocarbons were separated using a Restek RT-Msieve 5 A column (30 m × 0.32 mm with 0.03 mm film) and helium at

constant flow of 1.0 mL min^{-1} as carrier gas. The injection was performed in split mode with a split ratio of 1:50 at a temperature of 250 °C. Note that formaldehyde condensates to form dimethoxymethane at this injection temperature. The following oven temperature program was applied for the chromatographic separation: Initial temperature 35 °C isothermal for 4 min, heating up at a rate of 10 °C min^{-1} to 280 °C where temperature was kept constant for 16.5 min, resulting in an overall run time of 45 min. Retention times are listed in Table 2.

The MS was operated at standard EI parameters: 70eV collision energy, EM voltage of 1860 V, 230 °C MS source temperature. Data were acquired in selected ion monitoring (SIM) mode. The parameters used for the detection of the ions are listed in Table 2.

Gases included methane (puriss.; >99.995% (GC) from Fluka Analytical, Sigma Aldrich GmbH, Buchs, Switzerland), nitrogen (Carbagas, AG, Basel, Switzerland, grade 5.0), helium (Carbagas, AG, Basel, Switzerland, grade 5.0), argon (Carbagas, AG, Basel, Switzerland, grade 4.6) and a reference gas mixture (Westfalen AG, Münster, Germany) containing 94.8 ppm methane, 98.0 ppm ethane, 94.1 ppm propane, 101.0 ppm n-butane, 98.5 ppm ethane, 98.3 ppm acetylene and 96.2 ppm propene in nitrogen 5.0.

The reference gas mixture was diluted with helium in headspace vials to prepare calibration standards. These samples along with system suitability test (SST) samples were prepared as follows: 5 ml ultra-pure water were transferred into a pre-weighed 20 mL headspace vial (Infochroma, Zug, Switzerland) closed with a septum cap and purged for 5 min with helium. A 0.5 L gas sampling bag (SKC Limited, Dorset, UK) was evacuated for 5 min and filled with the 100 ppm reference gas mixture. The gas sampling bag was connected to the headspace vial by a stainless steel cannula. A 10 mL gas-tight syringe (Hamilton Bonaduz AG, Bonaduz, Switzerland) was used for gas transfer. For the calibration standards gas volumes of 0.25 mL, 0.5 mL, 1 mL, 2.5 mL, 5 mL, 7.5 mL, 10 mL and 12.5 mL were transferred into the headspace vial. For the SST samples a reference gas volume of 10 mL was transferred.

Table 2: Technical parameters for quantification of hydrocarbons, alcohols and aldehydes based on the method used (see text).

Compound	Retention Time R_f [min]	m/z
Butane	33	29,43,58
Ethane	13.5	27,29,30
Ethene	23.1	26,27,29,
Methane	3.6	15
Propane	23.4	26,27,29,43
Propene	31.3	39,41,42
Methanol	5.05	29, 31
Ethanol	6.22	31, 45, 46
1-Propanol	9.04	31, 59, 60
2-Propanol	7.16	45, 59
Formaldehyde [a]	4.14 + 7.05	29, 30, 75
Acetaldehyde	4.93	29, 31, 43
Propionaldehyde	6.90	29, 58, 59

[a] Formaldehyde: RF=4.14, m/z=29,30; Dimethoxymethane: RF=7.05, m/z=75

A similar procedure was applied to prepare samples from the batch corrosion experiments for GC-MS analysis. A gas sampling bag was evacuated for 5 min and filled with argon. The headspace vial was purged for 5 min with helium, closed and weighed. Samples from batch corrosion experiment were placed on a Neodym magnet to settle carbonyl-iron particles. Transfer of 5 mL supernatant solution into the prepared headspace vial was accomplished by using a 10 mL gas-tight syringe. The headspace vial was weighed to calculate the volume of the transferred solution.

3.2.2 Headspace Analysis of Alcohols and Aldehydes

Headspace samples (1 mL) were injected after 30 min incubation at 80 °C under agitation using a heated (85 °C) syringe. The analytes were separated using a Restek Rxi-624Sil MS column (60 m × 0.25 mm with 1.4 µm film) and helium at a constant flow of 1 mL/min as carrier gas. The injection was performed in split mode at a split ratio of 1:20. The temperature program was started at an initial temperature of 40 °C (for 1 minute) followed

by two ramps: first 5 °C min^{-1} up to 80 °C (for 1 minute) and then 20 °C min^{-1} to 200 °C resulting in a run time of 16 min. Retention times are listed in Table 2.

The MS was operated at standard EI parameters: 70eV collision energy, EM voltage of 1860 V, 230°C MS source temperature. Data were acquired in selected ion monitoring (SIM) mode. The parameters used for the detection of the ions are listed in Table 2.

Calibration of the analytes was performed using an analyte mixture, which was obtained from the pure single compounds. A 20 mL headspace vial (Infochroma, Zug, Switzerland) was filled with 5 mL of the calibration standard and analysed.

3.2.3 Analysis of Hydrocarbons in Gas Phase

Analysis of the hydrocarbons in the gas phase was performed with the equipment and GC-MS program previously described in Section 3.2.1. Gas samples were analysed using a headspace procedure and were injected from headspace vials.

At first, the gas samples were released into a gas sampling bag (0.5 L, SKC Limited, Dorset, UK) to achieve ambient pressure. Prior to analysis a headspace vial was twice evacuated and flushed with nitrogen. After the purging procedure 10 mL of the sample were taken from the gas sampling bag and injected into the purged and evacuated 20 mL headspace vial using a gas-tight syringe equipped with a valve (Hamilton Bonaduz AG, Bonaduz, Switzerland). Eventually, a second gas sampling bag filled with nitrogen was connected to the vial for 5 seconds to achieve pressure compensation in the sample vial.

For calibration, a gas sampling bag was filled with the reference gas mixture (see Section 3.2.1). Between 0.3 - 15 mL volume of the calibration gas was withdrawn (valve equipped gas-tight syringe, Hamilton Bonaduz AG, Bonaduz, Switzerland) and injected into a purged and evacuated 20 mL headspace vial. Prior to the headspace analysis pressure compensation in the vial was achieved using a second gas sampling bag filled with nitrogen, which was connected to the vial for 5 seconds.

3.3 *Results*

3.3.1 HPIEC-MS

Several criteria were used to assess the quality of the analytical method for the simultaneous analysis of the C1-C3 mono- and di-carboxylic aids, such as instrument and method linearity, ion suppression, recovery, precision, limit of detection and limit of quantification.

Linearity: The HPIEC method was calibrated over the concentration ranges listed in Table 3. As an example, typical calibration curves for acetic acid, ethanol and propane are shown in Figure 2. Linearity of the dynamic range was further tested by analyzing the standards of carboxylic acids in three different aqueous alkaline media (ACW I, ACW II, ACW III) at concentrations ranging between 10 to 200 µM (formic acid), 30 to 600 µM (acetic acid), 2.5 to 50 µM (malonic acid), 2.5 to 50 µM (oxalic acid), and 5 to 100 µM (valeric acid). The linearity of the method was assessed on the basis of the R^2 of the regression line obtained from the individual matrix-matched calibration solutions compared to those of ultra-pure water (Table 3).

Table 3: Instrument and method linearity for LMW organics tested in three different artificial cement pore waters [a].

Compound	Calibration range [µM]	Correlation R^2		
		ACW I	ACW II	ACW III
Acetic acid	0 - 200	0.994	0.993	0.999
Formic acid	0 - 600	0.999	0.995	0.996
Malonic acid	0 - 50	0.991	0.996	0.996
Oxalic acid	0 - 50	0.997	0.997	0.993
Valeric acid	0 - 100	0.998	0.993	0.998

[a] The compositions of the ACW solutions are given in Section 4.1.2 in Table 10.

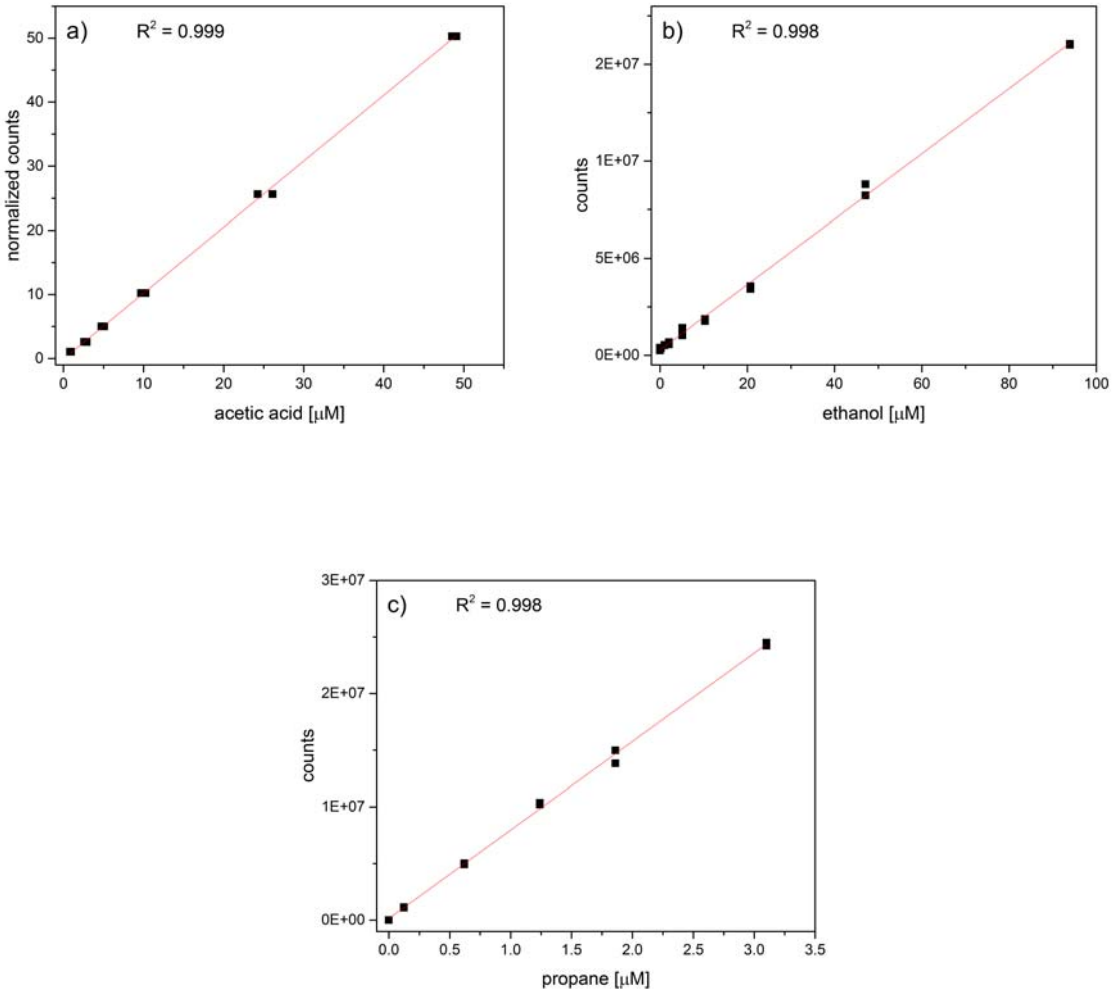

Figure 2: HPIEC-MS and GC-MS calibrations with standard compounds: a) HPIEC-MS of acetic acid, b) GC-MS of ethanol, c) GC-MS of propane from gas.

Signal suppression/enhancement: Matrix effects during analyte ionization give rise to suppression or enhancement of the analyte signal [Matuszewski *et al.*, 2003; Gosetti *et al.*, 2010]. In this study matrix effects were assessed by comparing the signal obtained from injection of the same amount of analyte in ultra-pure water (standard calibration curve) and a matrix-matched sample. Matrix effects (ME), i.e. signal suppression or enhancement, is expressed in percentage as follows:

$$ME(\%) = (s_{ACW}/s_{UPW})\cdot 100 \quad (1)$$

with s_{ACW} as the slope of the matrix-matched calibration curve and s_{UPW} as the slope of the curve for the standard calibration in ultra-pure water. If ME = 100% no matrix effect is observable while ME > 100 % corresponds to a signal enhancement and ME < 100 % corresponds to a signal suppression. Table 4 reveals that matrix effects are relatively small. It should be noted that the effect can be ignored if isotopic labeled internal standards (ILIS) are used in the analysis. The latter approach has been applied for all HPIEC measurements reported in this study.

Table 4: Matrix dependent ion suppression for LMW organics tested in three different artificial cement pore waters [a].

Compound	ME [%]		
	ACW I	ACW II	ACW III
Acetic acid	96%	104%	104%
Formic acid	99%	107%	120%
Malonic acid	109%	112%	104%
Oxalic acid	93%	111%	104%
Valeric acid	91%	104%	103%

[a] The compositions of the ACW solutions are given in Section 4.1.2 in Table 10.

Recovery, precision, limits of detection (LOD), limits of quantification (LOQ): Aqueous samples were spiked to obtain analyte concentrations of 10 to 200 µM, 30 to 600 µM, 2.5 to 50 µM, 2.5 to 50 µM, and 5 to 100 µM, respectively for formic acid, acetic acid, malonic acid, oxalic acid, and valeric acid. Five replicates for each concentration level were prepared. Three replicates of a non-spiked identical sample were analyzed simultaneously. The samples were pretreated using OnGuard® II Ag/H cartridges and injected in the HPIEC system. The recovery (REC) was determined from the five replicates as follows:

$$REC = (C_m/C_0)\cdot 100 \quad (\%) \qquad (2)$$

With C_m and C_0 as the determined and initial concentration of the analyte, respectively (Table 5).

Precision: The method precision (MP) was determined as the relative standard deviation of five subsequently analyzed replicates at the three different concentration levels of 10, 50, and 200 µM for formic acid, 30, 150, and 600 µM for acetic acid, 2.5, 12.5, and 50 µM for malonic acid, 2.5, 12.5, and 50 µM for oxalic acid, and 5, 25, and 100 µM for valeric acid. Similarly, the instrument precision (IP) was determined from five consecutive analyses of a single sample at concentration levels given above. In general it was found that IP ≤ MP and therefore MP is listed in Table 5. Furthermore, MP is typically < 15 % which is considered to be the uncertainty on the measurements.

Detection and quantification: The limit of detection (LOD) and the limit of quantification (LOQ) were estimated in accordance with definitions reported in the literature [Keith *et al.*, 1983; Barwick and Prichard, 2011]. LOD and LOQ were calculated as follows:

$$LOD = 3.3\cdot\sigma \qquad (3)$$

$$LOQ = 10\cdot\sigma \qquad (4)$$

The standard deviation σ was obtained from the results of the analysis of five replicates of sample containing the lowest quantifiable concentration of the analyte. LOD and LOQ values for the most important carboxylic acids are listed in Table 6.

3.3.2 GC-MS

Linearity of the GC-MS detection of the hydrocarbons (headspace, gas phase injection) and alcohols/aldehydes was checked over the concentration ranges given in Tables 7 and 8. Examples of the calibration curves of ethanol and propane are shown in Figure 2. The limit of detection (LOD) and the limit of quantification (LOQ) of the hydrocarbons and

alcohols/aldehydes were calculated using the ChemStation D.03.00.611 software to determine the standard deviation of the signal to noise ratio (S/N) of a sample at low concentration. The LOD and LOQ were estimated by multiplying the standard deviation by a factor of 3.3 or 10, respectively (Eqns. 3 and 4).

Table 5: Recovery and precision [a,b].

		Milli-Q		ACW I		ACW II		ACW III	
Compound	Conc. [µM]	REC [%]	MP [%]	REC [%]	MP [%]	REC [%]	MP [%]	REC [%]	MP [%]
Acetic acid	30	75	9	80	8	79	38	101	5
	150	103	8	105	6	99	6	106	5
	600	101	6	101	3	105	3	98	2
Formic acid	10	56	5	78	50	77	13	95	7
	50	61	11	100	9	96	11	104	2
	200	62	16	106	1	97	4	97	4
Malonic acid	2.5	99	6	92	2	64	3	44	11
	12.5	92	4	72	5	71	2	69	3
	50	103	3	90	3	71	3	82	3
Oxalic acid	2.5	72	8	133	10	n.d.	n.d.	85	5
	12.5	98	5	122	3	90	15	101	4
	50	96	8	105	8	106	6	95	3
Valeric acid	5	48	2	50	21	87	11	50	3
	25	106	5	97	9	94	16	110	3
	100	99	8	100	5	100	2	92	6

[a] The compositions of the ACW solutions are given in Section 4.1.2 in Table 10.
[b] REC: Recovery; MP: Method precision; n.d.: not determined

Table 6: Analytical parameters for quantification of the main carboxylic acids.

	Carboxylic acids		
Compound	**Formate**	**Acetate**	**Oxalate**
M [g/mol]	68.01	82.03	90.08
Calibration (min) [µM]	3	3	0.3
Calibration (max) [µM]	100	60	35
LOD [µM]	2	2	0.03
LOD [ppb]	136	164	2.7
LOQ [µM]	6	6	0.09
LOQ [ppb]	408	492	8.1

Table 7: Analytical parameters for the quantification of hydrocarbons.

	Hydrocarbons					
Compound	**Methane**	**Ethane**	**Ethene**	**Propane**	**Propene**	**Butane**
M [g/mol]	16.04	30.07	28.05	44.1	42.08	58.12
Calibration (min) [µM]	0.065	0.068	0.068	0.065	0.066	0.070
Calibration (max) [µM]	3.27	3.40	3.40	3.20	3.32	3.49
LOD [µM]	0.02	0.07	0.01	0.05	0.01	0.03
LOD [ppb]	0.32	2.10	0.28	2.21	0.42	1.74
LOQ [µM]	0.06	0.21	0.03	0.15	0.03	0.09
LOQ [ppb]	0.96	6.30	0.84	6.63	1.26	5.22

Table 8: Analytical parameters for the quantification of alcohols and aldehydes.

	Alcohols and Aldehydes						
Compound	**Meth-anol**	**Ethanol**	**1-Pro-panol**	**2-Pro-panol**	**Formal-dehyde**	**Acetal-dehyde**	**Propion-aldehyde**
M [g/mol]	32.04	46.07	60.10	60.10	30.03	44.05	58.08
Calibration (min) [µM]	11	8	0.6	0.6	2	0.1	0.06
Calibration (max) [µM]	240	163	128	125	40	67	12
LOD [µM]	0.6	2.5	0.5	0.04	1.6	0.2	0.04
LOD [ppb]	19	115	30	2.4	48	9	2.3
LOQ [µM]	1.8	7.5	1.5	0.12	4.8	0.6	0.12
LOQ [ppb]	57	445	90	7.2	144	27	6.9

4 Determination of the Carbon Species Formed from Corrosion Experiments with Non-activated Iron Powders

Studies on the corrosion of inactive iron powders were carried out with the aim of identifying the carbon species formed under anoxic alkaline conditions. The study included measurements of carbon release both to the gas phase and the liquid phase. The latter phases were analysed using the HPIEC-MS and GC-MS analytical methods described in Section 3. Knowledge of the organic compounds formed in corrosion experiments with non-activated iron powders is essential for the development of advanced analytical methods aiming at determining the ^{14}C containing compounds that are expected to be released at much lower concentration in the course of the corrosion of activated steel.

4.1 *Materials and Methods*

4.1.1 Iron Powders

Two different carbonyl-iron powders (carbonyl-iron powder (SIGMA), Sigma-Aldrich GmbH Buchs, Switzerland, and BASF-HQ (BASF), BASF Ludwigshafen, Germany) were used for the corrosion experiments. Both powders were produced by the reduction of $Fe(CO)_5$ by hydrogen. The carbonyl-iron powders were pretreated using a procedure described elsewhere [Deng *et al.*, 1997] with the aim of removing surface contaminants remaining from the manufacturing process. Briefly, the powders were immersed for 30 min in N_2-purged 1.0 N hydrochloric acid (HCl). Thereafter, they were rinsed 15 times with N_2-purged water, and dried under a N_2 atmosphere at 100 °C. The powders were stored in the glove box in N_2 atmosphere prior to use. The treatment yielded grayish colored iron powders.

Both powders consist of spherical particles with diameters in the range of a few microns (Figure 3). The difference in size is reflected by their difference in the average surface area which was determined from N_2 sorption measurements on four replicates using a Micromeritics Gemini VII 2390 analyzer (Micromeritics GmbH, Aachen, Germany) (Table 9). The diameter of 90 % of the particles (d(90)) was found to be d(90) ~ 2.2 µm [Wanner,

2007] for the BASF powder and d(90) ~ 3.1 µm (estimated based on surface areas) for the Sigma product. Thus, the particle sizes of the two products are slightly different.

Scanning electron microscopy (SEM) with microanalysis (EDX) of the untreated carbonyl-iron powders showed that the particles consist of pure iron, suggesting that the content of impurities, e.g. other metals, is negligible (Figure 4, Table 9). The carbon and nitrogen contents are relatively high, i.e. slightly below 1 %.

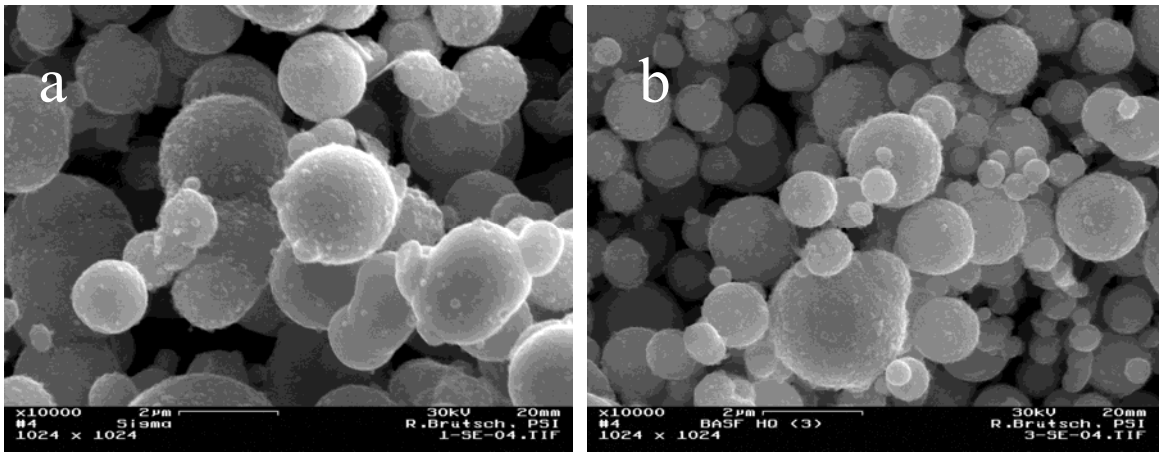

Figure 3: SEM images of the two different carbonyl-iron powders a) SIGMA powder, and b) BASF powder.

Table 9: Summary of the morphological and physical properties of the used carbonyl-iron powders in the anaerobic corrosion experiments and microanalysis (EDX) data.

Iron powder	Fe content [%]	C content [%]	N content [%]	Surface area [m^2/g][a]
SIGMA untreated	99.6 ± 0.7 [b]	0.83 [d]	n.d.	0.44 ± 0.03
SIGMA pretreated	n.d.	n.d.	n.d.	0.73 ± 0.05
BASF-HQ untreated	98.2 ± 0.8 [b]	0.7-0.9 [c]	0.9 [c]	0.87 ± 0.07
BASF-HQ pretreated	n.d.	n.d.	n.d.	1.73 ± 0.09

[a] determined by Micromeritics GmbH, Aachen, Germany
[b] determined with SEM-EDX
[c] data from supplier: BASF, Ludwigshafen, Germany
[d] [Deng *et al.*, 1997]
n.d.: not determined

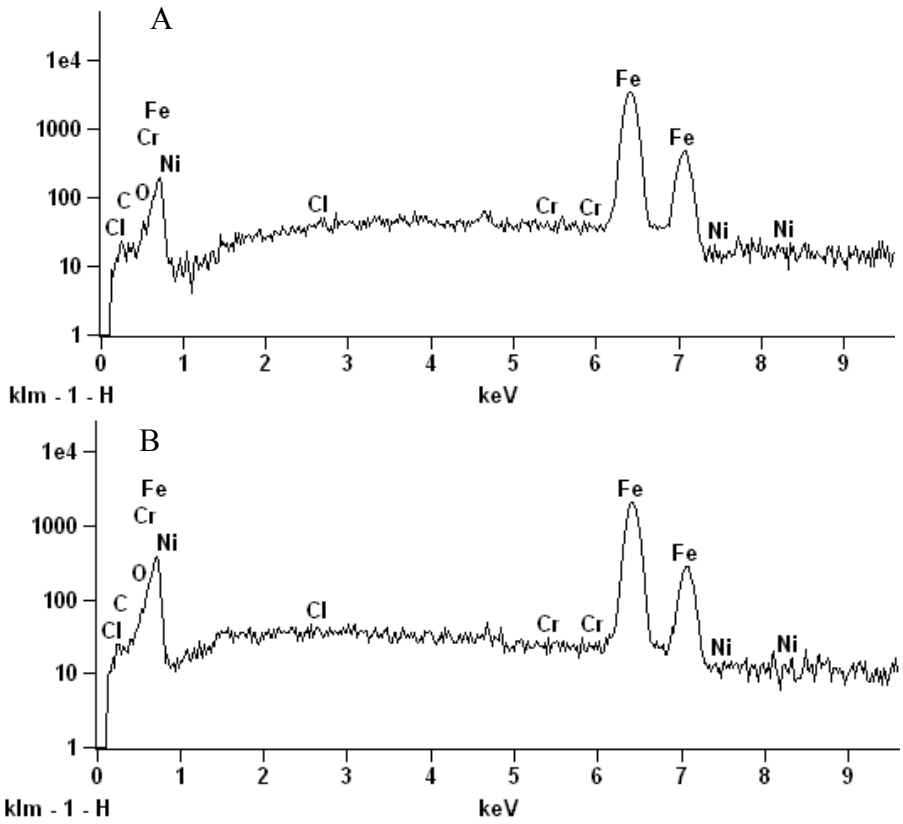

Figure 4: Microanalysis (EDX) data pictures for the two different carbonyl-iron powders using a Zeiss DSM 962 SEM microscope. A) SIGMA powder, and B) BASF-HQ powder.

4.1.2 Solutions

Throughout this study the solutions were prepared using Fluka or Merck "pro analysis" (analytical-grade) chemicals. Deionized, decarbonated water (Milli-Q water; 18.2 MΩ*cm) was generated by a Milli-Q Gradient A10 purification system (Millipore, Bedford, MA, USA), which was used for the preparation of solutions and standards.

Three different artificial cement pore water (ACW) solutions at pH 11.0 (ACW I), 12.5 (ACW II), and 13.3 (ACW III) were prepared using analytical-grade chemicals and deaerated Milli-Q water. The latter water was prepared by acidifying Milli-Q water to pH 4.0 using HCl and subsequent boiling for 30 min under continuous N_2 purge. Afterwards, the water bottle was tightly sealed and transferred into a glovebox with N_2 atmosphere.

The ACW solutions correspond to different stages of the cement degradation in the course of the service life of a repository. ACW III is an alkali containing pore water in equilibrium with "fresh" cement paste. The solution had the composition as given in Table 10 and was prepared according to a procedure described elsewhere [Wieland *et al.*, 2006]. ACW II is a portlandite-saturated solution and corresponds to a solution in equilibrium with cement paste degraded to the stage II of the cement degradation (Table 10). The solution was prepared as follows: $Ca(OH)_2$ was fired at 1000°C until constant weight to produce CaO. 2 g CaO was mixed with 1 L degassed Milli-Q water, shaken end-over-end for at least two days in the glovebox with N_2 atmosphere. After checking the pH, the suspension was filtered using a 100 nm polyethersulfone membrane filter (Criticap-MTM, Gelman Science, USA). ACW I corresponds to a solution in equilibrium with a calcium silicate hydrate (C-S-H) phase with Ca/Si (C/S) ratio = 0.8, which was prepared according to a procedure described in detail elsewhere [Tits *et al.*, 2014]. Briefly, 0.0481 g AEROSIL 300 (SiO_2) (Evonik Industries, AG, Germany) and 0.0449 g CaO were mixed with 1 L deaerated Milli-Q water in polyethylene bottles. The suspension was shaken end-over-end for at least 2 weeks in the glove box. After checking the pH, the suspension was filtered and the filtrate was stored in the glovebox until use.

Table 10: Composition of the aqueous solutions used in the batch corrosion experiments.

Element	ACW I [mol/L]	ACW II [mol/L]	ACW III [mol/L]
Na	n.d.	n.d.	$1.2 \cdot 10^{-1}$
K	n.d.	n.d.	$1.8 \cdot 10^{-1}$
Al	n.d.	n.d.	$5.0 \cdot 10^{-5}$
Ca	$8.0 \cdot 10^{-4}$	$2.0 \cdot 10^{-2}$	$1.6 \cdot 10^{-3}$
Cl	n.d.	n.d.	$1.0 \cdot 10^{-4}$
Si	$8.0 \cdot 10^{-4}$	n.d.	$2.0 \cdot 10^{-5}$
pH	11.0	12.5	13.3

n.d.: not detected

4.1.3 Methods

4.1.3.1 Scanning Electron Microscopy (SEM) with Microanalysis (EDX)

The SEM/EDX analysis was carried out using a Zeiss DSM962 microscope operated at an accelerator voltage of 30 kV. The microscope is equipped with a Si(Li)-detector for EDX. The spot size area was approximately 1 × 1µm^2 with a penetration depth of ~ 6 µm at the incident beam energy. The carbonyl iron powders were fixed on a specimen holder (Al, Ø = 12.5 mm, Plano GmbH, G301) and coated with gold using the high current evaporation method. Images were obtained at the highest magnification of 10'000x of the microscope.

4.1.3.2 pH and Eh Measurements

The pH was measured using a LL-Aquatrode electrode (Metrohm, Zofingen, Switzerland), which was calibrated to the pH_c scale using KOH solutions (0.001 M, 0.01 M, 0.02 M, 0.05 M, 0.1 M) prepared from 1 M KOH titrisol.

Eh measurements were carried out using a Mikro-Pt-Titrode 16 OK electrode (Metrohm, Zofingen, Switzerland) calibrated with a redox buffer (Eh = 250 ± 5 mV at 20 ºC).

The pH and Eh measurements were carried out as follows: The vials containing the iron suspensions were left on a strong Neodym magnet (40 × 40 × 20 mm, supermagnete.ch) over night to accelerate and complete removal of the iron particles by sedimentation. The pH and Eh electrodes were immersed in the supernatant solution. The indicated values were recorded after 15 min at the latest or after obtaining constant readings, respectively.

4.1.3.3 Elemental Analysis

The total concentrations of the main elements in the supernatant (Na, K, Ca, Al, Si, Fe) were determined by plasma emission spectroscopy using an Applied Research Laboratory ARL 3410D inductively coupled plasma optical emission spectrometer (ICP-OES). 5 mL aliquots of the supernatants were acidified with 0.2 mL HNO_3 65 % and diluted with Milli-Q water to a total volume of 25 mL.

4.1.3.4 HPIEC-MS and GC-MS Analyses

The carboxylates were determined using the HPIEC-MS method previously described in Section 3.1. Hydrocarbons and alcohols/aldehydes were determined using the headspace method for GC-MS previously described in Sections 3.2.1 and 3.2.2.

All samples analyzed by HPIEC-MS were pretreated using OnGuard® II Ag/H cartridges (Dionex/Thermo Fisher, Sunnyvale, CA, USA) to remove interfering Cl^- ions and protonate OH^-. Prior to use the cartridges were conditioned in 10 mL ultra-pure water. Approximately 10 mL of each sample were passed through the cartridge, of which the first 4 mL were discarded. 0.75 mL of the remaining solutions were collected for HPIEC analysis, spiked with 50 µL of the ILIS mix and stored at 4 °C in the refrigerator. The samples were analyzed within 48 h after preparation.

The samples from the batch corrosion experiments were prepared for GC-MS analysis as follows. The headspace vial was purged for 5 min with helium, closed and weighed. The samples from the batch corrosion experiments were placed on the Neodym magnet to retain the carbonyl-iron particles. Transfer of 5 mL solution into the prepared headspace vial was accomplished using a 10 mL gas-tight syringe. The headspace vial was weighed to record the volume of the transferred solution.

4.1.3.5 Experimental Protocol

For the time-dependent corrosion experiments 20 mL headspace vials (Infochroma, Zug, Switzerland) containing 1.0 g carbonyl-iron powder were filled with one of the alkaline ACW solutions (no gas headspace) in the glovebox and sealed. To this end, a teflon strip was pulled over the thread of the vial, and the cap was screwed onto the vial. Blank samples were filled solely with the respective alkaline solution. All vials were placed in a plastic box impermeable to light, which was mounted onto an end-over-end shaker. The batch-type corrosion experiments were carried out in a glovebox (CO_2 and O_2 < 2ppm). Samples were taken after 1, 2, 7, 14, 21, 28, and 35 days, respectively, and analyzed (two reaction and one control bottle) using HPIEC-MS and GC-MS.

So-called exchange experiments were carried out as follows: 20 mL headspace vials (Infochroma, Zug, Switzerland) containing 1.0 g carbonyl-iron powder were filled with one of the alkaline ACW solutions (no gas headspace) in the glovebox and sealed. In one series of exchange experiments the alkaline solution was replaced sequentially three times in the same vials which had been equilibrated for 3 days between the replacements. In the other series of exchange experiments the alkaline solution was withdrawn from the first iron-containing vial and injected into the second vial containing fresh iron powder. Three replacements were carried out successively and the samples were equilibrated for 3 days between the replacements. The samples were analysed using HPIEC-MS and GC-MS.

4.2 *Results*

4.2.1 Chemical Conditions in the Batch-type Experiments

The redox potential, pH and the concentrations of the main elements were monitored over the time span of the corrosion experiments using the pretreated BASF HQ powder immersed in the alkaline solutions (Figure 5, Table 11). In ACW II pH was buffered as expected at 12.5 and further, as expected for an iron-water systems, conditions were strongly reducing (Eh = -520 ± 9 mV). This indicates absence of oxygen in the samples. In ACW I, however, pH dropped from initially 11.0 to 9.1 ± 0.4 while conditions were also strongly reducing (Eh = -549 ± 13 mV), thus indicating absence of oxygen. The time-dependent development of pH and Eh was not monitored in the iron-ACW III systems because we anticipate a similar behaviour as in the case of the iron-ACW II system, i.e. buffered pH and a negative Eh value. Furthermore, we expect the same chemical conditions in samples with the pretreated Sigma iron powders.

Table 11: Time dependence of pH, Eh and the main elements in the iron-ACW I and iron-ACW II systems during corrosion of pretreated BASF powder.

Solution	Time [d]	pH	Eh [mV]	Ca [mg/L]	Si [mg/L]	Fe [mg/L]
ACW I*	1	8.76	-537	30.4	0.29	5.81
	2	8.74	-530	30.5	0.19	11.30
	7	9.39	-539	29.9	0.40	2.10
	14	9.67	-558	28.3	0.92	1.11
	21	9.52	-555	29.2	0.82	0.86
	28	8.81	-556	30.3	0.36	6.16
	35	9.31	-568	29.9	0.82	1.45
ACW II*	1	12.52	-500	805	0.35	0.65
	2	12.49	-520	802	0.42	1.70
	7	12.49	-528	792	0.40	1.97
	14	12.48	-529	787	0.59	0.91
	21	12.48	-523	769	0.50	0.47
	28	12.50	-519	760	0.50	1.59
	35	12.47	-520	757	0.52	1.65

* Initial pH: ACW I: pH = 11; ACW II: pH = 12.5

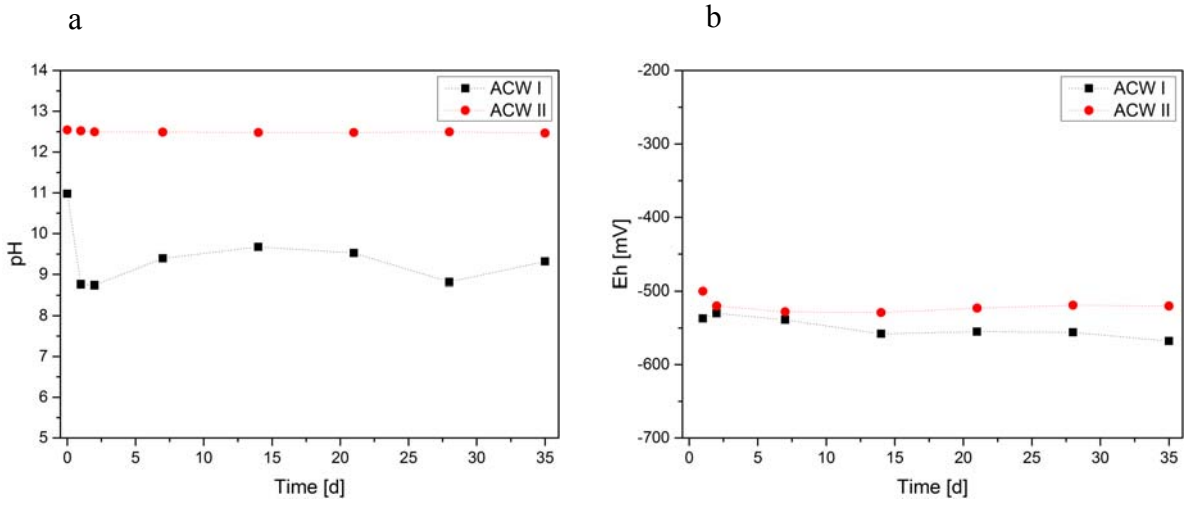

Figure 5: Time dependence of pH (a) and Eh (b) in iron-ACW I and iron-ACW II samples.

The pH drop in the pretreated iron-ACW I system (pH = 11 → pH ~ 9) seems to be caused by the dissolution of a small amount of iron oxides initially present on the surface of the iron powders [Diomidis, 2014]. In aerated solutions steel corrosion occurs and produces an iron oxyhydroxide according to:

$$4\ Fe + 3\ O_2 + 2\ H_2O \rightarrow\ 4\ FeOOH \qquad (5)$$

FeOOH represents a stoichiometry intermediate between Fe_2O_3 (oxide) and $Fe(OH)_3$ (hydroxide). Note that iron oxyhydroxides may have been produced during pretreatment of the iron powders. Nevertheless, the composition of the surface oxide layer is expected to be more complex and may consists of several sub-layers such as an inner magnetite layer and outer hematite films [Diomidis, 2014; Swanton *et al.*, 2014]. The specific reaction conditions such as the amount of available oxygen, the availability and composition of water, the hydration conditions and the reaction kinetics determine the mineral composition of the oxide layer. For the following considerations it is assumed that FeOOH is a surrogate for the corrosion products formed during pretreatment. The main mechanisms in the early stage of the corrosion process involves the reduction of the FeOOH to Fe_3O_4 (magnetite) which was given for acidic conditions as follows [Diomidis, 2014]:

$$2\ FeOOH + Fe^{2+} \rightarrow Fe_3O_4 + 2\ H^+ \qquad (6)$$

Equation (6) reveals that the conversion of the oxyhydroxide into magnetite produces protons which neutralizes alkalinity in solution. Note that an equivalent reaction holds in alkaline conditions where aqueous Fe(II) hydroxide is the dominant species. Mass balance calculations indicate that a pH_c drop from 11 to 9.1 (± 0.4) can be attributed to the conversion of $9.87 \cdot 10^{-4}$ (± $0.1 \cdot 10^{-4}$) mol FeOOH. The total amount of Fe in the samples (1 g Fe powder) was $1.79 \cdot 10^{-2}$ mol Fe. Thus, the change in alkalinity suggests that ~ 5.5 % (± 0.1 %) Fe was oxidized to FeOOH in the pretreatment process and rapidly dissolved in the first stage of the corrosion process. Semi-quantitative SEM/EDX analysis on a few points of interest revealed oxygen contents ranging between 1.3 – 3 wt.-%, thus supporting the presence of iron oxides on the iron particles.

Once the oxyhydroxide is reduced the anoxic corrosion of iron is considered to occur according to the following reaction (e.g. [Diomidis, 2014]):

$$3\ Fe + 4\ H_2O \rightarrow Fe_3O_4 + 2\ H_2 \qquad (7)$$

In this study gas formation, presumably the production of H_2, was observed in the samples and limited the time period over which headspace-free conditions were achieved.

4.2.2 Time-dependent Release of Organic Compounds

Time-dependent release of the conjugate bases of carboxylic acids and hydrocarbons is shown for the iron-ACW I and iron-ACW II systems using pretreated BASF powder (Figures 6 and 7) and for the iron-ACW I and iron-ACW II systems using pretreated Sigma-Aldrich powder (Figures 8 and 9). Time-dependent formation of the organic compounds was further determined for the untreated Sigma-Aldrich powder immersed in ACW solutions. The results are summarized in the Appendix (Table A 3).

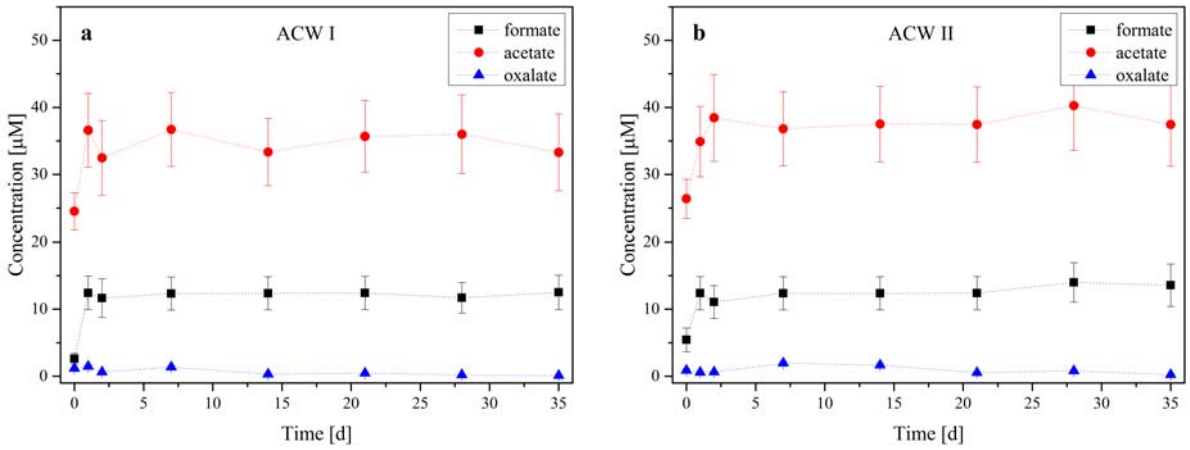

Figure 6: Time-dependent release of carboxylate ions in the iron-ACW I (a) and iron-ACW II (b) systems during corrosion of pretreated BASF powder.

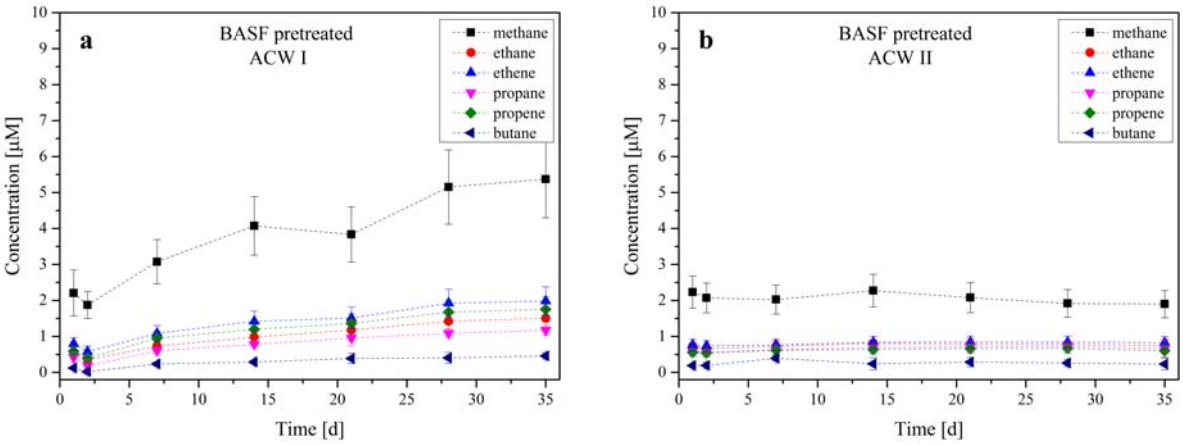

Figure 7: Time-dependent release of hydrocarbons in the iron-ACW I (a) and iron-ACW II (b) systems during corrosion of pretreated BASF powder.

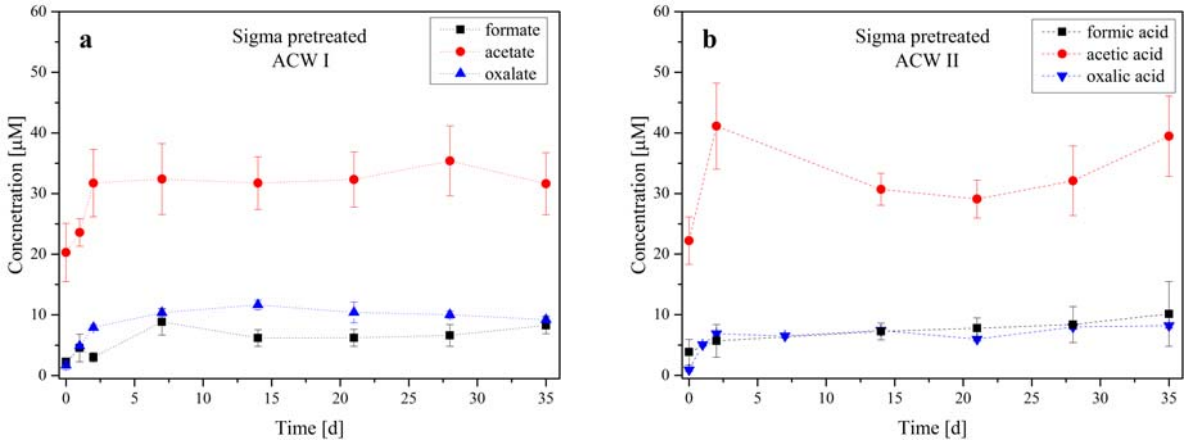

Figure 8: Time-dependent release of carboxylate ions in the iron-ACW I (a) and iron-ACW II (b) systems during corrosion of pretreated Sigma-Aldrich powder.

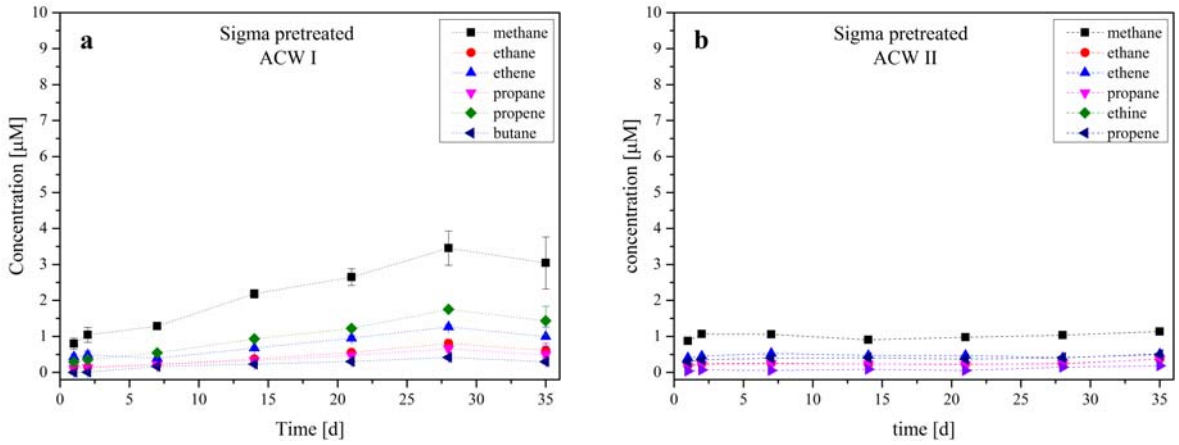

Figure 9: Time-dependent release of hydrocarbons in the iron-ACW I (a) and iron-ACW II (b) systems during corrosion of pretreated Sigma-Aldrich powder.

Formate, acetate and oxalate were identified as the only conjugate bases of carboxylic acids formed at significant concentrations during corrosion of the iron powders in ACW I and ACW II. Lactate, propanoate, butanoate and malonate were detected but at concentrations close to the detection limit (concentrations below LOQ are not listed). The formation of organic compounds with a high molecular weight, however, can be excluded based on the results from this study. Note that also in the earlier studies, the presence of large molecules was not observed [Wieland and Hummel, 2015]. The concentration of acetate was determined to be ~ 35 µM in all iron-ACW systems containing either the pretreated BASF or the pretreated Sigma-Aldrich powder, respectively. The concentration of formate was lower than that of acetate in all these systems, i.e. ranging between ~ 5 - 15 µM (Tables A1 and A2 in Appendix). In the case of oxalate, however, the concentration was found to be lower in the iron-ACW systems containing the pretreated BASF powder, i.e. ranging between ~ 0.1 - 1.9 µM, while the concentration of oxalate was similar to that of formate in the iron-ACW systems containing the pretreated Sigma-Aldrich powder, i.e. ranging between ~ 1 - 12 µM. In ACW III (pH = 13.3) the concentrations of formate and acetate were found to be below the detection limit while the oxalate concentration ranged between ~ 0.5 - 7.9 µM (Tables A1 and A2 in Appendix). Also, for all iron-ACW systems, formate and acetate could not be detected in the samples containing the untreated Sigma-Aldrich powder while the oxalate concentrations ranged between ~ 1.3 - 13 µM (Table A3 in Appendix).

Thus, it appears that the concentrations of formate and acetate are much lower in the iron-ACW systems containing the untreated Sigma-Aldrich powder than in those containing the pretreated powders while pretreatment did not affect the oxalate concentration.

In all iron-ACW systems we were able to detect methane, ethane, ethene, propane, propene and butane (Figures 7 and 9). No other hydrocarbons were observed. The concentrations of the hydrocarbons increased with time in the iron-ACW I systems containing either pretreated Sigma-Aldrich or BASF powder, respectively, indicating progressive corrosion. In the iron-ACW II systems, however, the concentrations of all hydrocarbons were constant due to a combination of low rate of corrosion at high pH and the short experimental duration. The concentrations ranged in value between ~ 0.2 - 2.3 μM. On the basis of mean concentrations the following order of concentration was observed for the iron-ACW II systems containing the pretreated iron powders: methane > ethane ~ ethene ~ propane ~ propene > butane. In the iron-ACW III systems we also observed constant concentrations over time as in the case of the iron-ACW II system and the above approximate order with respect to the concentration of the hydrocarbons (Tables A1 and A2 in Appendix). No major difference in the concentration level was further observed between the iron-ACW systems containing either untreated or pretreated Sigma-Aldrich powders, respectively. Nevertheless, the steady increase in the concentrations was less pronounced in the iron-ACW I system containing the untreated Sigma-Aldrich iron powder.

We also identified alcohols and aldehydes formed in the iron-ACW I and iron-ACW II systems containing the pretreated BASF iron powder (Table 12). In general, the concentrations were found to be close to the LOQ for all compounds. In particular, the concentrations were lower than those of the carboxylic acids indicating that alcohols and aldehydes are only minor compounds formed during the anoxic corrosion of the iron powder.

Table 12: Time-dependent release of alcohols and aldehydes in the iron-ACW I and iron-ACW II systems during corrosion of pretreated BASF powder.

		Alcohols and aldehydes [µM]			
Solution	**Time [d]**	**Methanol**	**Ethanol**	**Formaldehyde**	**Acetaldehyde**
ACW I	1	< 1.8	< 7.5	< 4.8	0.6 ± 0.2
	2	< 1.8	< 7.5	< 4.8	0.9 ± 0.3
	7	< 1.8	< 7.5	< 4.8	1.5 ± 0.4
	14	< 1.8	< 7.5	< 4.8	1.1 ± 0.3
	21	< 1.8	< 7.5	< 4.8	0.9 ± 0.3
	28	< 1.8	< 7.5	< 4.8	1.1 ± 0.3
	35	< 1.8	< 7.5	5.3 ± 0.7	1.3 ± 0.4
ACW II	1	n.d.	8 ± 2	5.4 ± 0.9	0.9 ± 0.3
	2	< 1.8	8 ± 2	5.5 ± 0.9	0.9 ± 0.3
	7	< 1.8	< 7.5	< 4.8	<0.6
	14	< 1.8	8 ± 2	5.8 ± 0.8	0.8 ± 0.2
	21	< 1.8	9 ± 2	5.9 ± 0.7	0.7 ± 0.2
	28	< 1.8	7 ± 2	5.4 ± 0.6	0.6 ± 0.2
	35	< 1.8	8 ± 2	5.9 ± 0.6	0.6 ± 0.2

n.d.: not detected

4.2.3 Instantaneous Release of Organic Compounds

The aforementioned studies on the time-dependent evolution of the concentrations of organic compounds indicated that, in all cases, the release of both hydrocarbons and carboxylate ions was very fast upon contacting the iron powders with alkaline solution. In addition, a series of exchange experiments were carried out aiming at illustrating fast release in the very early stage of the corrosion process. The experiments were based on sequential, multiple replacement of the ACW solution in a sample containing 1 g iron powder (total 4 exchange cycles). The samples were equilibrated between solution replacements for 3 days. The concentration of the carboxylate ions and hydrocarbons was high in the solution initially added to the iron powder (Figure 10). However, the solutions of the following exchange cycles had significantly lower concentrations. Fast release of both carboxylate ions and hydrocarbons indicates the presence of very reactive carbon species at the surface

of the iron powders which are released upon contact with ACW solutions. Note that both classes of compounds show similar behaviour.

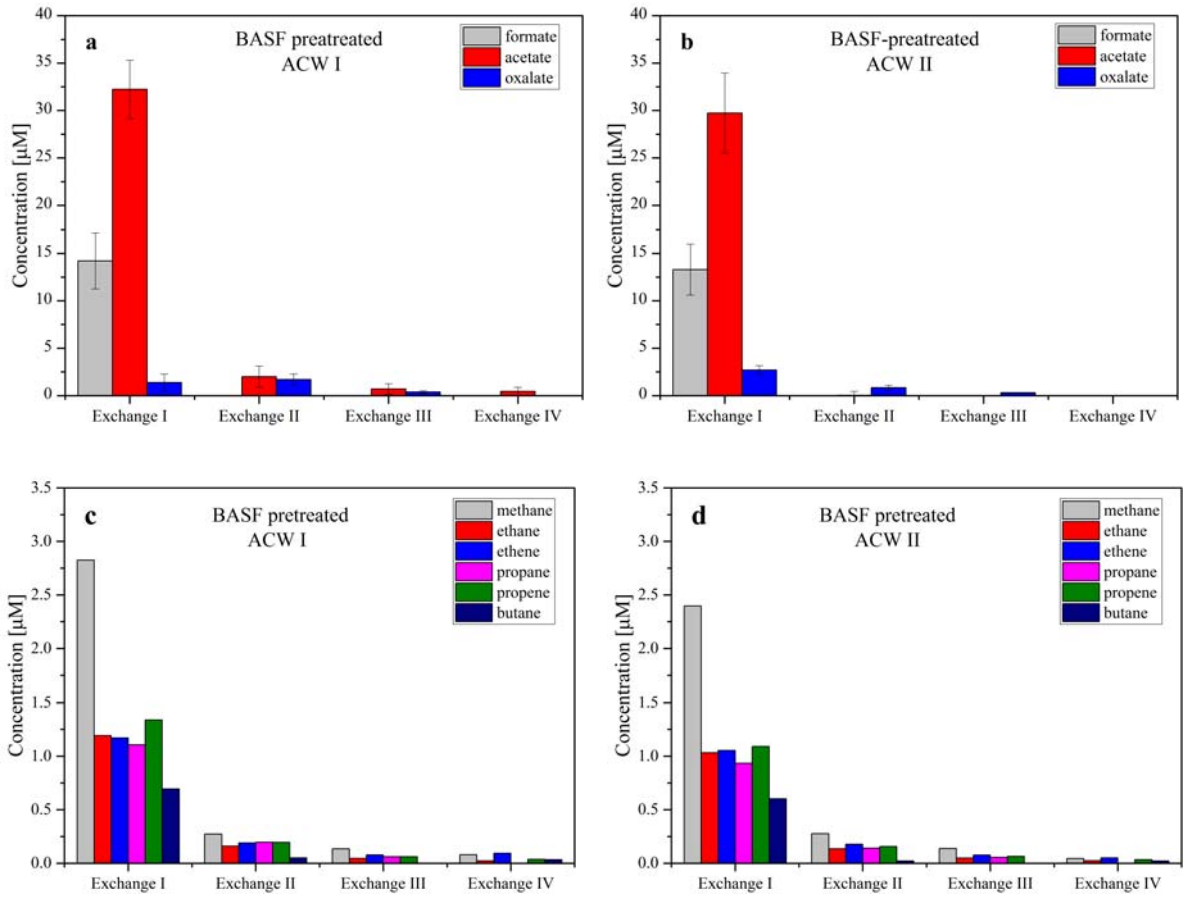

Figure 10: Concentrations of carboxylate ions and hydrocarbons in the exchange experiments (equilibration time = 3 days). a) carboxylate ions in ACW I/pretreated BASF samples, b) carboxylate ions in ACW II/pretreated BASF samples, c) hydrocarbons in ACW I/pretreated BASF samples, d) hydrocarbons in ACW II/pretreated BASF samples.

A series of short-term experiments using an equilibration time of 0.5 min were carried out in order to compare instantaneous release of the organic compounds in pretreated and un-

treated iron powders (Figure 11). Instantaneous release of the carboxylate ions was observed in case of the pretreated iron powders immersed in ACW I, and ACW II while their concentrations were below the LOD in case of the untreated Sigma-Aldrich powder. Note again that, in the latter case, very small amounts of oxalate could be detected. These results indicate that significant release of the carboxylate ions, except oxalate, only occurs in case the iron powder had been pretreated. This finding implies that significant amounts of formate and acetate were formed during pretreatment of the iron powders and were accommodated in the oxidic surface layer of the iron particles. Oxalate, however, could already be present in the commercial iron powder as an impurity (untreated Sigma-Aldrich iron powder).

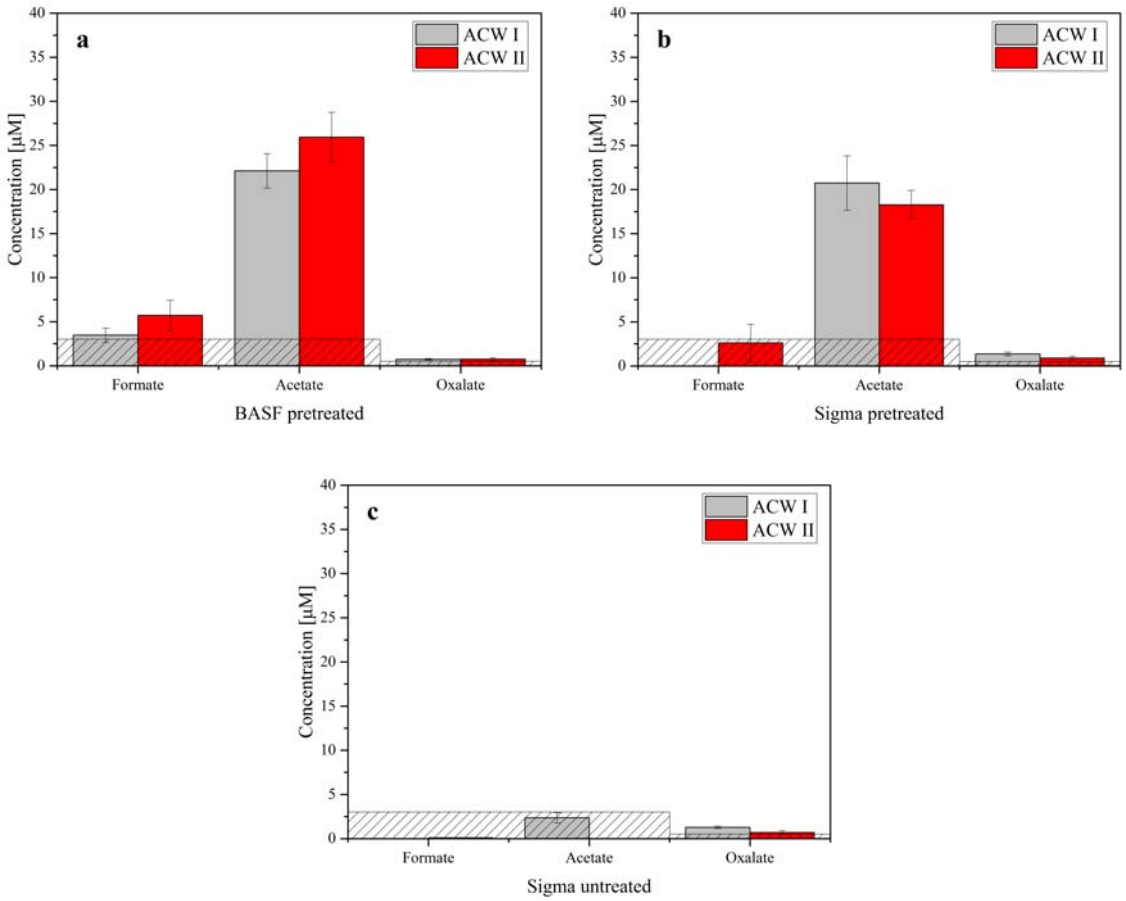

Figure 11: Instantaneous release of carboxylate ions (equilibration time = 0.5 min) by pretreated BASF (a), pretreated Sigma-Aldrich (b) and untreated Sigma-Aldrich (c) iron powder.

We also checked the formation of hydrocarbons in the short-term experiments. The concentrations of the hydrocarbons were found to be below the LOD, except in the case of methane where small amounts were detected (data not shown). The concentration of the volatile organic compounds in these short-term experiments is expected to be very small as the reaction time is short and corrosion is slow.

In summary, the release of carboxylate ions to solution is significantly faster in the first minutes upon contacting the pretreated iron powders with ACW solutions compared to the release of gaseous hydrocarbons while a similar release pattern was observed over longer equilibration times. This finding suggests that the reactivity of the carbon species at the surface of the iron powders is different, which further implies that either the concentration of the reactive surface species or the kinetics of the reactions that lead to the formation of carboxylate ions and gaseous hydrocarbons are different.

4.2.4 Formation of the Organic Compounds

Two possible processes are conceivable that give rise to simultaneous formation of oxidized and gaseous hydrocarbons in the experiments:

I. The formation of the carboxylate ions and gaseous hydrocarbons occurs simultaneously as a consequence of two different reactions, i.e. oxidation and reduction, occurring on the iron surface. This implies that carboxylate ions are formed by the oxidation of carbon (either graphite (C(0)), carbide (Fe_3C,) or other reduced intermediates such as methylene and methyl species on the iron surface [Kaminsky *et al.*, 1986]. Oxidation requires the presence of residual oxygen dissolved in solution in the samples. In contrast, hydrocarbons would form on the strongly reducing iron surface by a Fischer-Tropsch analogous process [Deng *et al.*, 1997].

II. The release of carboxylate ions and the formation of hydrocarbons are the consequence of two very different processes. The oxidized carbon species were formed during the pretreatment process (oxidizing conditions) and accommodated in the oxide layer of the iron particles. In contact with water,

conversion of the oxide layer into magnetite occurred according to equation (6) which releases the carboxylate ions retained in the oxide layer. This is a very fast process as indicated from the pH drop that occurred within one day in the iron-ACW I system (pH = 11 → pH ~9; Table 11). Hence, the two processes, i.e. instantaneous release of carboxylate ions (Figures 10 and 11) and pH drop, which was observed in the iron-ACW I system but not in the buffered iron-ACW II (Table 11) and iron-ACW III systems, coincide in the very early stage of the corrosion process. In contrast, the formation of gaseous hydrocarbons would again take place on the strongly reducing iron surface due to the reduction of carbon species bound on the surface by a process related to the Fischer-Tropsch synthesis.

It should be noted that the exchange experiments described in Section 4.2.3 suggest different kinetics of the two reactions, i.e. the formation of carboxylate ions and hydrocarbons. The release of carboxylate ions to solution seems to be faster than the formation and release of hydrocarbons.

We performed a series of additional exchange experiments with the aim of checking the above hypotheses. The key to distinguishing between the two hypotheses is whether or not residual oxygen was present in the ACW solutions in the exchange experiments. In case of oxygen-free solution simultaneous oxidation and reduction of carbon species on the surface of the iron particles can be excluded. The new series of exchange experiments was carried out in a fashion similar to those previously described in Section 4.2.3. In the latter experiments fresh solution was subsequently added to the same iron powder. In the new series of experiments, however, we subsequently added the same solution to several samples containing iron powder as follows: ACW solution was added to the first vial containing iron powder. After equilibration for 3 days the solution was withdrawn from the first vial using a gas-tight syringe and injected in the second vial containing fresh iron powder. Sample manipulations were done in the glovebox under a N_2 atmosphere to avoid any contamination with oxygen. We expect that residual oxygen dissolved in ACW is consumed by an oxidation process on the surface of the iron powder in the first vial. Hence, after 3 days of

equilibration, the ACW solution should be free of oxygen. Injecting the oxygen-free solution into the second vial containing fresh iron powder allows the two possible processes of carboxylate release to be discriminated. The concentration of carboxylate ions should not increase in solution if oxidation were the dominant process generating the carboxylate ions. However, an increase in the concentration of carboxylate ions is anticipated if the compounds formed during pretreatment of the iron powders were accumulated in the oxide layer of the iron powders and were released to solution upon conversion of the oxide layer into magnetite. Figure 12 shows the results from the tests carried out in ACW I. The concentration of the carboxylate ions gradually increases by successively adding the same solution to different vials containing fresh iron powder. This shows that the formation of carboxylate ions by an oxidation process can be ruled out.

4.3 *Discussion*

A survey of corrosion studies revealed that the number of carbon-containing compounds formed in the course of the anoxic corrosion of iron and steel is limited [Wieland and Hummel, 2015]. The compounds that have been reported in literature are listed in Table 13. Development of the analytical methods in the framework of this study (GC-MS, HPIEC-MS) was based on the assumption that all these organic compounds could form during corrosion of the iron powders. Most compounds reported in the literature have been observed in the corrosion experiments carried out in this study. The compounds identified in this study are highlighted in bold in Table 13. In addition, presence of lactate was observed at concentrations close to the LOD (listed as bold italic table entry). Nevertheless, we were not able to detect butylenes and pentene. It should be noted that the concentration of carbonate that could form is limited by $CaCO_3$ solubility in alkaline conditions. The presence of large amounts of $CaCO_3$ was not observed indicating that carbonate presumably is a minor inorganic carbon species formed during iron corrosion. Table 13 shows that only small molecules up to C5 form during corrosion. In particular, experimental evidence for the formation of high molecular weight organic compounds is lacking. Thus, the present study supports previous results that only a limited number of LMW organic compounds form in the course of the anoxic corrosion of iron and steel.

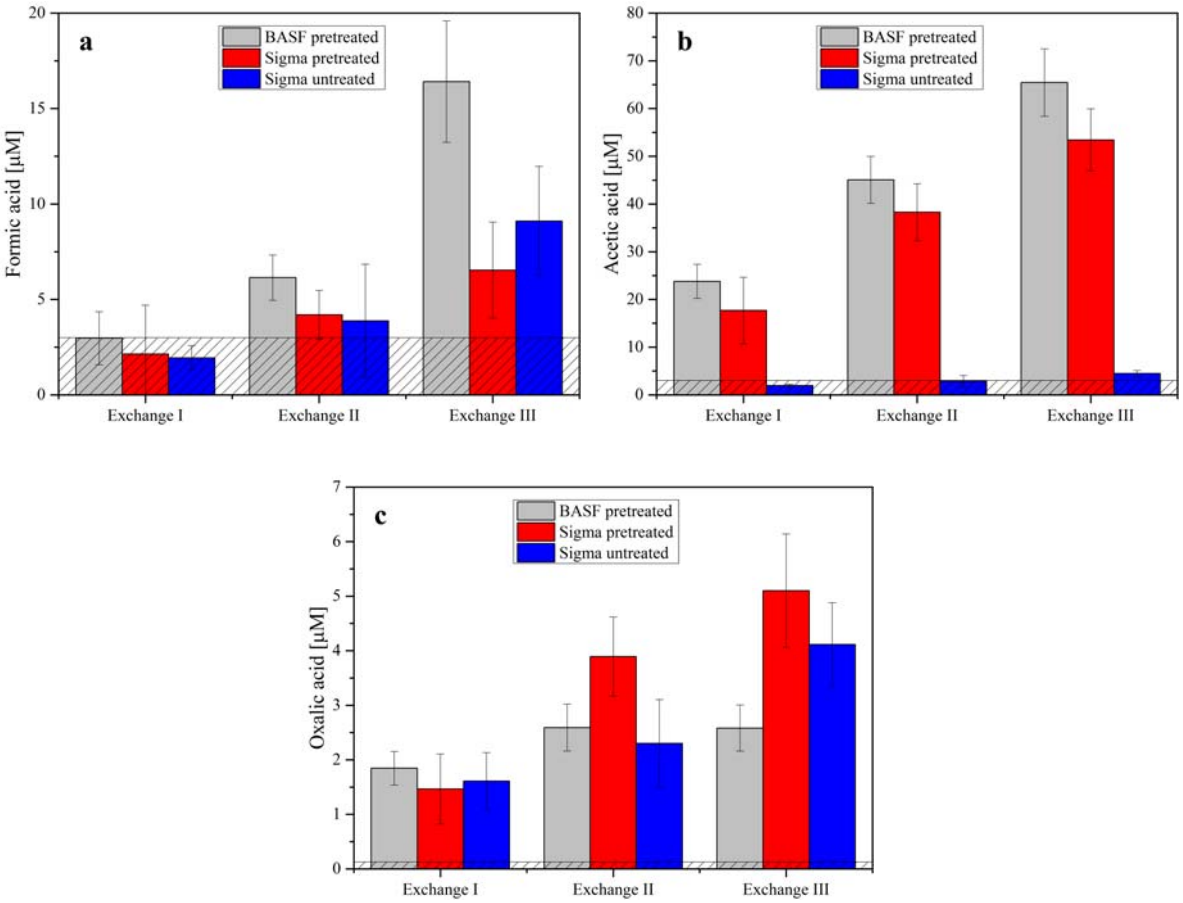

Figure 12: Concentrations of carboxylate ions in the exchange experiments (equilibration time = 3 days) adding the same ACW I solution successively to vials containing fresh iron powder. a) formate, b) acetate, c) oxalate. The concentrations of other carboxylate ions was < LOQ.

Table 13: Carbon species expected to form as a result of steel corrosion as reported in literature (all table entries except lactate) and subsequently identified in this study (highlighted in bold and bold italic).

Alkane/alkene	Alcohols/aldehydes	Carboxylate ions	Carbonate
Methane (CH_4)	**Methanol** (CH_3OH)	**Formate** ($HCOO^-$)	CO_2
Ethane (C_2H_6)	**Ethanol** (C_2H_5OH)	**Acetate** (CH_3COO^-)	CO_3^{2-}
Ethene (C_2H_4)	**Formaldehyde** (CH_2O)	**Propanoate** ($C_2H_5COO^-$)	(CO)
Propane (C_3H_8)	**Acetaldehyde** (C_2H_4O)	**Butanoate** ($C_3H_7COO^-$)	
Propene (C_3H_6)	**Propionaldehyde** (C_3H_6O)	**Malonate** ($CH_2(COO^-)_2$)	
Butane (C_4H_{10})		**Oxalate** ($C_2O_4^{2-}$)	
Butylene (C_4H_8)		***Lactate*** *($CH_3CHOHCOO^-$)*	
Pentene (C_5H_{10})			

A previous review of corrosion studies points to the apparent contradiction in the current understanding of the carbon speciation in corrosion studies [Wieland and Hummel, 2015; Swanton *et al.*, 2014]. The formation of hydrocarbons from the hydrolysis of certain metal carbides is well known and in accordance with the notion that reducing conditions prevail at the iron-water interface. In contrast, the well-documented presence of oxidised water-soluble carbon species demands further explanation. The results from this study corroborate the presence of oxidised carbon species in corroding iron-water systems in anoxic conditions, in particular the presence of formate, acetate and oxalate while alcohols and aldehydes are only minor species. However, the study also shows that the anoxic corrosion does not give rise to the release of oxidized hydrocarbons. The presence of oxidized hydrocarbons is the consequence of a preceding corrosion process of iron in oxic conditions and the uptake of these oxidised species by the oxide layer. In the first stage of the anoxic corrosion of iron the oxide layer is converted to magnetite which releases the oxidised carbon species to solution. It appears that the oxidised species are chemically stable under the given conditions or reduction is slow, respectively, and therefore not detectable over the 35 days reaction time considered in this study. Hence, after instantaneous release, the concentration of the oxidised species was found to be constant with time. The release of the oxidised species occurs almost instantaneous when iron is immersed in alkaline solution in anoxic conditions indicating that conversion of the oxide layer to magnetite is fast.

Mass balance calculations enable us to determine the total concentration of oxidised carbon species that might be released in the initial stage of anoxic corrosion. The content of iron oxide/oxyhydroxide on the surface of iron particles was estimated at ~ 5.5 wt.-% on the basis of the pH drop in the iron-ACW I system (pH = 11 → pH = 9.1) caused by the conversion of iron oxyhydroxide to magnetite. The concentration of carbon in the BASF iron powder amounts to ~ 0.9 wt.-% (range: 0.7 - 0.9 wt.-%). Thus, in the samples containing 1 g pretreated BASF iron powder the amount of oxidised iron amounts to ~ 55 mg Fe which corresponds to ~ $4.1 \cdot 10^{-5}$ mol total carbon. This further corresponds to a maximum carbon concentration of ~ $2.1 \cdot 10^{-3}$ M that could build up in solution. From the experimental data listed in Tables A1 and A2 it is estimated that the total concentration of

carbon associated with the main oxidised species in the aqueous phase, i.e. formate (1 C), acetate (2 C) and oxalate (2 C), amounts to ~ $8.5 \cdot 10^{-5}$ M. This indicates that only a small portion of carbon in the iron oxyhydroxide layer was in fact oxidized and accommodated as formate, acetate or oxalate, respectively (~ 4 %).

The formation of hydrocarbons supports the idea that gaseous carbon species are the main compounds formed under the strongly reducing conditions at the iron-water interface. The concentration of the hydrocarbons increases with time in ACW I (pH = 9.1) while constant concentrations were determined in ACW II (pH = 12.5). Note that corrosion of the iron powders was comparable in ACW II (pH = 12.5) and ACW III (pH = 13.3). This finding is in line with the current understanding of corrosion processes in alkaline media. Corrosion of iron and steel is extremely slow in strongly alkaline conditions (< 10 nm a^{-1}) while rates increase with decreasing pH [Diomidis, 2014; Swanton *et al.*, 2014].

The release of gaseous hydrocarbons is also very fast in the initial stage of the corrosion process (< 3 days) which is attributed to the presence of very reactive carbon species on the iron surface. Fast production of hydrocarbons was observed in both ACW I and ACW II (as well as in ACW III). For longer reaction times up to 35 days, however, the release of hydrocarbons is significantly decelerated. The increase in the concentration of gaseous hydrocarbons observed in ACW I (pH = 9.1) over the time period up to 35 days allows a corrosion rate to be estimated based on carbon release (Figure 13). The corrosion rate for the pretreated BASF iron powder was determined to be ~ 0.16 uM C d^{-1} excluding the potentially faster initial reaction and taking into account the formation of hydrocarbons between 7 and 35 days. This results in an estimated Fe release rate of ~ 3.8 uM Fe d^{-1} based on the initial stoichiometry of Fe and C in the iron powder (Fe:C = 23:1) and on the assumption that stoichiometric release of Fe and C occurred in the corrosion experiment. Eventually, the Fe release rate, which is based on the C release rate, can be converted into a corrosion rate as follows:

$$R = \frac{M \cdot k}{A_s \cdot m_{Fe} \cdot \rho} \qquad (m\ d^{-1}) \qquad (8)$$

M: Molar mass of Fe (= 0.05585 kg mol^{-1})

k: Fe release rate (= $3.84 \cdot 10^{-3}$ mol m^{-3} d^{-1})

A_s: Specific surface area of iron powder (= $1.8 \cdot 10^{3}$ m^2 kg^{-1})

m_{Fe}: Mass of iron powder in sample (= 50 kg m^{-3})

ρ: Density of iron (= 7855 kg m^{-3})

The corrosion rate was estimated at $3.0 \cdot 10^{-13}$ m d^{-1} which corresponds to an annual corrosion rate of $1.1 \cdot 10^{-10}$ m a^{-1} (= 0.1 nm a^{-1}) at pH ~9. Note that this value is unexpectedly low compared to those determined on the basis of volumetric H_2 measurements in near-neutral conditions [Diomidis, 2014; Swanton *et al.*, 2014].

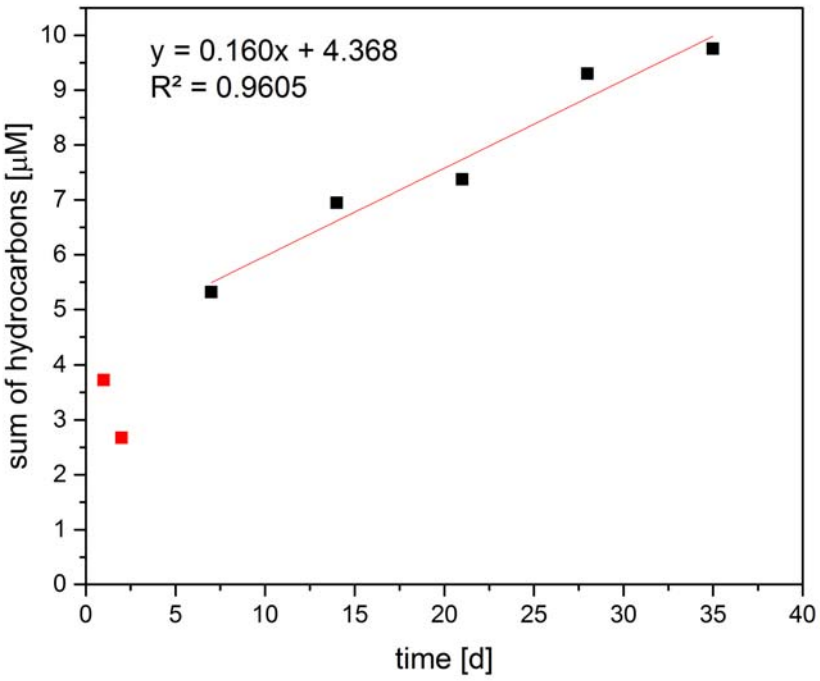

Figure 13: Corrosion rate determined based on carbon release in ACW I (pH = 9.1).

5 Development of a Compound-specific ^{14}C AMS Analytical Technique

Preliminary calculations showed that the concentrations of ^{14}C bearing organic compounds expected to be formed in the planned corrosion experiments with the available activated steel sample are extremely low (see Section 2.2.5). The main constraints are 1) the low ^{14}C inventory of the activated steel (~ 18 kBq g^{-1}; [Schumann *et al.*, 2014]), 2) a low corrosion rate of steel under hyper-alkaline conditions (typically < 50 nm a^{-1}) and 3) the low amount of material that can be used in corrosion experiment with activated steel due to the high dose rate of the activated steel (~ 20 mSv g^{-1} h^{-1}; [Schumann *et al.*, 2014]). As indicated in Section 2.2.5 the ^{14}C concentration in samples that had been subjected to chromatographic separation of single compounds might be well below 10^{-18} mol ^{14}C. Therefore, detection of very low ^{14}C concentrations requires an extremely sensitive ^{14}C analytical method. To this end, a compound-specific ^{14}C AMS technique is currently being developed based on the coupling of standard separation techniques (GC, HPIEC) with ^{14}C detection by AMS.

5.1 *^{14}C Analysis with AMS*

5.1.1 AMS Facility at the University of Bern

The accelerator mass spectrometer (AMS) MICADAS (MIni CArbon DAting System) shown in Figure 14 became operational in May 2013 in the Laboratory for Environmental and Radiochemistry at the University of Bern [Szidat *et al.*, 2014]. Substantial technical developments in accelerator mass spectrometry has allowed the breakthrough of the small device MICADAS [Synal *et al.*, 2007]. The instrument is comparable in terms of precision and detection limit with large AMS systems with the advantage of requiring only small amounts of sample material at short process time. Furthermore, the simplified instrumental set-up reduces running costs and service efforts compared to large AMS systems. The ion source allows targets of solid graphite and gaseous carbon dioxide to be used. The automated gas interface reported by [Wacker *et al.*, 2013a] enables the transfer of carbon dioxide to the gas ion source from different sources, such as sealed glass ampoules, an

acidification device for carbonate samples [Wacker *et al.*, 2013b], an elemental analyzer [Ruff *et al.*, 2010] or other combustion instruments [Perron *et al.*, 2010].

Detection limits and performance of the MICADAS were reported by [Szidat *et al.*, 2014].

5.1.2 Data Presentation

In conventional atomic mass spectrometry, samples are atomized and ionized, separated by their mass-to-charge ratio, then measured and/or counted by a detector. Rare isotopes such as ^{14}C present a challenge to conventional MS due to their low natural abundance and high background levels.

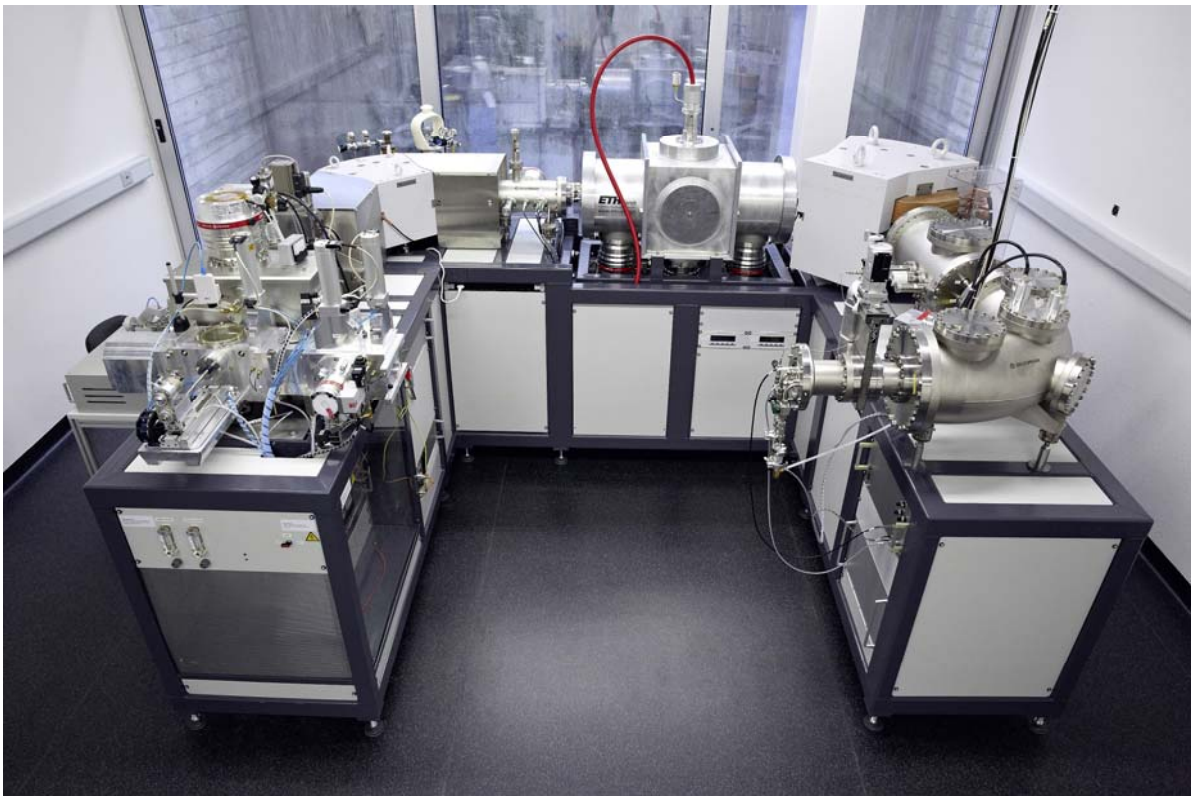

Figure 14: Mini Carbon Dating System (MICADAS) at the Laboratory for Environmental and Radiochemistry at the University of Bern (Switzerland)

The main challenges in ^{14}C measurements are isobaric interference (interference from equal mass isotopes of different elements exemplified by ^{14}N in ^{14}C analysis), isotopic

interference (interference from equal mass to charge isotopes of different elements), and molecular interference (interference from equal mass to charge molecules, such as $^{12}CH_2^-$, $^{12}CD^-$, or $^{13}CH^-$ in ^{14}C analysis). Most AMS systems employ an electrostatic tandem accelerator that has a direct improvement in background rejection, resulting in a 10^8 time increase in the sensitivity of isotope ratio measurements. As the natural abundance of ^{14}C in modern carbon is about 10^{-12} (isotopic ratio of ^{14}C:^{12}C), a sensitivity of 10^{-15} is a prerequisite for ^{14}C analysis. The $^{14}C/^{12}C$ ratio is given in units of fraction modern (fm) or as a percentage of Modern Carbon ($F^{14}C$):

$$1F^{14}C = \frac{^{14}C}{\left(^{12}C \times 1.18 \cdot 10^{-12}\right)} \qquad (9)$$

Note that modern is roughly equivalent to $9.8 \cdot 10^{-17}$ mol ^{14}C mg^{-1} ^{12}C.

5.2 *HPIEC Separation and ^{14}C Detection by AMS for Aqueous Compounds*

5.2.1 Analytical Approach

A schematic illustration of the analytical approach that we are currently developing is outlined in Figure 1. Compound-specific ^{14}C AMS analysis of aqueous samples collected from the reactor involves several subsequent steps briefly outlined as follows.

Separation and fraction collection: Aliquots of the sampled solution are spiked with a standard solution containing ^{14}C-free ^{12}C carrier of the compounds that are subjected to ion chromatographic separation (see method described in Section 3.1). The concentration of the compounds is chosen in a way that MS detection is possible with the aim of controlling chromatographic separation. The chromatographically separated, individual compounds are sampled by a fraction collector. Carbon-12 carrier is added to the latter samples to obtain the total carbon content required for ^{14}C AMS (20 µg total carbon). The samples are stored in the freezer prior to measurements.

On-line measurement: An elemental analyzer is used as combustion unit for direct radiocarbon measurements of small samples (10 µL sample with 20 µg ^{12}C). The elemental analyzer is connected to an external trap for enrichment and integrated in the gas inlet system of the AMS [Ruff *et al.*, 2010]. Small aliquots of the solution are transferred into small capsules and combusted at 950 ºC in a helium atmosphere temporarily enriched with oxygen. Complete oxidation is achieved by a CuO catalyst prior to separation of the gaseous combustion products. CO_2 leaving the elemental analyzer in a helium stream is selectively enriched on an external trap containing X13 zeolite absorber material. The trap can be heated up from room temperature to 500 ºC in 40 s, which releases CO_2 to the gas injection system (see details in [Ruff *et al.*, 2010]). The external trap is sensitive to cross-contamination, which has to be quantified in the framework of this project.

5.2.2 Outlook

PSI intends to develop a compound-specific ^{14}C AMS analytical technique for liquid samples in the framework of the ongoing EC project "CAST" focussing on the identification and quantification of the compounds listed in Table 13. The analytical development is undertaken in a systematic manner along the following steps:

1. Recovery, repeatability and precision of the separation by IC and fraction collection using ^{12}C compounds

2. Systematic evaluation of the ^{14}C background in the corrosion reactor and in the course of the chromatographic separation in combination with ^{14}C AMS measurements (e.g. solutions, IC separation, transport to AMS etc.)

3. Determination of the dynamic range of the ^{14}C AMS using ^{14}C containing acetic acid

4. Recovery, repeatability and precision of the separation by IC and fraction collection using ^{14}C containing single compounds (Table 13) and mixes of these ^{14}C containing compounds

5. Assessment of cross-contamination in ^{14}C AMS measurements

5.3 GC Separation and ^{14}C Detection by AMS for Gaseous Compounds

5.3.1 Analytical Approach

The analytical approach that we are currently developing for the determination of ^{14}C containing compounds is schematically shown in Figure 1. Compound-specific ^{14}C AMS analysis of gaseous samples collected from the reactor involves several steps, similar to those previously described for the aqueous samples, as follows.

Separation and fraction collection: Hydrocarbons, alcohols and aldehydes can be determined using the headspace procedure. Small aliquots of the aqueous solution are spiked with a standard gas mixture containing ^{14}C-free ^{12}C carrier of the compounds that are subjected to GC separation (see method described in Section 3.2). The concentration of the compounds is chosen in a way that thermal conductivity detection (TCD) is possible with the aim of controlling chromatographic separation. The chromatographically separated, individual compounds are oxidized by a combustion reactor to CO_2 and trapped by the fraction collector. The trapping valves of the fraction collector are pre-loaded with ^{14}C-free CO_2 to achieve the total amount of carbon required for ^{14}C AMS (20 µg total carbon). A similar approach is applied for the gaseous samples in which hydrocarbons will be separated and oxidized prior to ^{14}C AMS measurement.

The coupling of the GC to the combustion reactor with fraction collector is currently under development.

On-line measurement: The trapping valves can be connected to the gas inlet system with integrated external trap for enrichment [Ruff *et al.*, 2010]. $^{14}CO_2$ is injected into the ^{14}C AMS via the gas inlet system.

5.3.2 Outlook

PSI intends to develop a compound-specific ^{14}C AMS analytical technique for the detection of ^{14}C containing volatile compounds, such as hydrocarbons, alcohols and aldehydes, in the framework of the ongoing EC project "CAST". These compounds are also listed in Table 13. The analytical development requires the same aspects as previously outlined for the analysis of ^{14}C containing aqueous compounds to be dealt with in a systematic manner:

1. Recovery, repeatability and precision of the separation by GC and fraction collection using ^{12}C compounds

2. Systematic evaluation of the ^{14}C background in the corrosion reactor and during chromatographic separation in combination with ^{14}C AMS measurements

3. Recovery, repeatability and precision of the GC separation coupled to combustion and fraction collection using ^{14}C containing single compounds and mixes of these ^{14}C containing compounds

4. Assessment of cross-contamination in ^{14}C AMS measurements

6 References

AGRAWAL, A., FERGUSON, W. J., GARDNER, B. O., CHRIST, J. A., BANDSTRA, J. Z., TRATNYEK, P. G. 2002. Effects of carbonate species on the kinetics of dechlorination of 1,1,1-trichloroethane by zero-valent iron. *Environmental Science & Technology,* 36(20), 4326-4333.

ALLARD, B., TORSTENFELT, B., ANDERSSON, K. 1981. Sorption studies of $H^{14}CO_3^-$ on some geological media and concrete. *Material Research Society Symposium Proceedings,* 3, 465-473.

Nuclear Decommissioning Authority 2012. Geological disposal. Carbon-14 Project - Phase 1 Report, NDA/RWMD/092.

BARWICK, V.J., PRICHARD, E. (Eds) 2011. Eurachem Guide: Terminology in Analytical Measurements - Introduction to VIM 3 (2011). *Eurachem*, ISBN 978-0-948926-29-7 (available from www. eurachem.org).

BAYLISS, S., EWART, F. T., HOWSE, R. M., SMITH-BRIGGS, J. L., THOMASON, H. P., WILLMOTT, A. 1988. The solubility and sorption of lead-210 and carbon-14 in a near-field environment. *Material Research Society Symposium Proceedings,* 112, 33-42.

CAMPBELL, T. J., BURRIS, D. R., ROBERTS, A. L., WELLS, J. R. 1997. Trichloroethylene and tetrachloroethylene reduction in a metallic iron-water-vapor batch system. *Environmental Toxicology and Chemistry,* 16(4), 625-630.

CHI, G. T., HUDDERSMAN, K. D. 2007. Novel ion chromatography technique for the rapid identification and quantification of saturated and unsaturated low molecular weight organic acids formed during the Fenton oxidation of organic pollutants. *Journal of Chromatography A,* 1139(1), 95-103.

DENG, B. L., BURRIS, D. R., CAMPBELL, T. J. 1999. Reduction of vinyl chloride in metallic iron-water systems. *Environmental Science & Technology,* 33(15), 2651-2656.

DENG, B. L., CAMPBELL, T. J., BURRIS, D. R. 1997. Hydrocarbon formation in metallic iron/water systems. *Environmental Science & Technology,* 31(4), 1185-1190.

DIOMIDIS, N. 2014. Scientific basis for the production of gas due to corrosion in a deep geological repository. Nagra, Wettingen, Switzerland, NAB 14-21.

FISCHER, K., HOEFFLER, S., MEYER, A. 2006. Systematic examination of the signal area precision of a single quadrupole enhanced low mass option (ELMO) TSQ (TM) mass spectrometer. *Rapid Communications in Mass Spectrometry,* 20(16), 2419-2426.

GLAUS, M. A., VAN LOON, L. R., ACHATZ, S., CHODURA, A., FISCHER, K. 1999. Degradation of cellulosic materials under the alkaline conditions of a cementitious repository for low and intermediate level radioactive waste Part I: Identification of degradation products. *Analytica Chimica Acta,* 398(1), 111-122.

GOSETTI, F., MAZZUCCO, E., ZAMPIERI, D., GENNARO, M.C. 2010. Signal suppression/enhancement in high-performance liquid chromatography tandem mass spectrometry, *Journal of Chromatography A*, 1217, 3929-3937.

HARDY, L. O., GILLHAM, R. W. 1996. Formation of hydrocarbons from the reduction of aqueous CO_2 by zero-valent iron. *Environmental Science & Technology,* 30(1), 57-65.

JOHNSON, L., SCHWYN, B. 2008. Proceedings of a Nagra/RWMC Workshop on the Release and Transport of C-14 in Repository Environments, NAB 08-22, Nagra, Wettingen, Switzerland.

KAMINSKY, M. P., WINOGRAD, N., GEOFFROY, G. L., VANNICE, M. A. 1986. Direct SIMS observation of methylidyne, methylene, and methyl intermediates on a Ni(111) methanation catalyst. *Journal of the American Chemical Society,* 108(6), 1315-1316.

KANEKO, S., TANABE, H., SASOH, M., TAKAHASHI, R., SHIBANO, T., TATEYAMA, S. 2003. A study on the chemical forms and migration behavior of carbon-14 leached from the simulated hull waste in the underground condition. *Materials Research Society Symposium Proceedings*. 757, 621-626.

KANI, Y., NOSHITA, K., KAWASAKI, T., NASU, Y., NISHIMURA, T., SAKURAGI, T., ASANO, H. 2008. Decomposition of C-14 containing organic molecules released from radioactive waste by gamma-radiolysis under repository conditions. *Radiation Physics and Chemistry,* 77(4), 434-438.

KEITH, L. H., CRUMMETT, W., DEEGAN, J., LIBBY, R. A., TAYLOR, J. K., WENTLER, G. 1983. Principles of environmental analysis, *Analytical Chemistry,* 55(14), 2210-2218.

MATSUMOTO, J., BANBA, T., MURAOKA, S. 1995. Adsorption of carbon-14 on mortar. *Materials Research Society Symposium Proceedings,* 353, 1029-1035.

MATUSZEWSKI, B.K., CONSTANZER, M.L., CHAVEZ-ENG, C.M. 2003. Strategies for the assessment of matrix effect in quantitative bioanalytical method based on HPLC-MS/MS, *Analytical Chemistry* 75, 3019-3030.

NAGRA 2002. Project Opalinus Clay: Safety report. Demonstration of disposal feasibility for spent fuel, vitrified high-level waste and long-lived intermediate-level waste (Entsorgungsnachweis). Nagra, Wettingen, Switzerland, NTB 02-05.

NOSHITA, K. 2008. Fundamental study of C-14 chemical form under irradiated condition in *Proceedings of a Nagra/RWMC workshop on the release and transport of C-14 in repository environments*, JOHNSON, L and SCHWYN, B. (editors), Nagra, Wettingen, Switzerland, NAB 08-22, 65 - 70.

NOSHITA, K., NISHI, T., MATSUDA, M., IZUMIDA, T. 1996. Sorption mechanism of carbon-14 by hardened cement paste. *Materials Research Society Symposium Proceedings,* 412, 435-442.

PERRON, N., SZIDAT, S., FAHRNI, S., RUFF, M., WACKER, L., PREVOT, A. S. H., BALTENSPERGER, U. 2010. Towards on-line C-14 analysis of carbonaceous aerosol fractions. *Radiocarbon,* 52(2), 761-768.

POINTEAU, I., COREAU, N., REILLER, P. 2003. Etude experimentale et modélisation de la rétention de 14CO32- par les matériaux constituant le béton dans le cadre des études de faisabilité d'un stockage de déchets graphites. Andra, Paris, France, FRP 18 CEA 03-001.

RUFF, M., FAHRNI, S., GÄGGELER, H. W., HAJDAS, I., SUTER, M., SYNAL, H. A., SZIDAT, S., WACKER, L. 2010. On-line radiocarbon measurements of small samples using elemental analyzer and MICADAS gas ion source. *Radiocarbon,* 52(4), 1645-1656.

SASOH, M. 2008a. Investigations of distribution coefficients for C-14 from activated metal in *Proceedings of a Nagra/RWMC workshop on the release and transport of C-14 in repository environments*, JOHNSON, L and SCHWYN, B. (editors), Nagra, Wettingen, Switzerland, NAB 08-22, 83-86.

SASOH, M. 2008b. Study on chemical behaviour of organic C-14 under alkaline conditions in *Proceedings of a Nagra/RWMC workshop on the release and transport of C-14 in repository environments*, JOHNSON, L and SCHWYN, B. (editors), Nagra, Wettingen, Switzerland, NAB 08-22, 79 - 82.

SASOH, M. 2008c. The study for the chemical forms of C-14 released from activated steel in *Proceedings of a Nagra/RWMC workshop on the release and transport of C-14 in repository environments*, JOHNSON, L and SCHWYN, B. (editors), Nagra, Wettingen, Switzerland, NAB 08-22, 21-23.

SCHUMANN, D., STOWASSER, T., VOLMERT, B., GUENTHER-LEOPOLD, I., LINDER, H., WIELAND, E. 2014. Determination of the C-14 content in activated steel components from a neutron spallation source and a nuclear power plant. *Analytical Chemistry,* 86(11), 5448-5454.

SMART, N. R., BLACKWOOD, D. J., MARSH, G. P., NAISH, C. C., O'BRIEN, T. M., RANCE, A. P., THOMAS, M. I. 2004. The anaerobic corrosion of carbon and stainless steel in simulated cementitious repository environments: A summary review of Nirex Research. AEA Technology, Harwell, United Kingdom, AEAT/ERRA-0313.

SWANTON, S. W., BASTON, G. M. N., SMART, N. S. 2014. Rates of steel corrosion and carbon-14 release from irradiated steel - state of the art review. CAST WP2 Deliverable 2.1.

SYNAL, H.-A., STOCKER, M., SUTER, M. 2007. MICADAS: A new compact radiocarbon AMS system. *Nuclear Instruments & Methods in Physics Research Section B-Beam Interactions with Materials and Atoms,* 259(1), 7-13.

SZIDAT, S., SALAZAR, G. A., VOGEL, E., BATTAGLIA, M., WACKER, L., SYNAL, H.-A., TÜRLER, A. 2014. C-14 analysis and sample preparation at the new Bern Laboratory for the analysis of radiocarbon with AMS (LARA). *Radiocarbon,* 56(2), 561-566.

TAKAHASHI, R., SASOH, M., YAMASHITA, Y., TANABE, H., SAKURAGI, T. 2014. Improvement of inventory and leaching rate measurements of C-14 in hull waste, and separation of organic compounds for chemical species identification. *Materials Research Society Symposium Proceedings,* 1665, 139-148.

TITS, J., FUJITA, T., HARFOUCHE, M., DÄHN, R., TSUKAMOTO, M., WIELAND, E. 2014. Radionuclide uptake by calcium silicate hydrates: Case studies with Th(IV) and U(VI). Paul Scherrer Institute, Villigen PSI, Switzerland, PSI Report 14-03.

WACKER, L., FAHRNI, S. M., HAJDAS, I., MOLNAR, M., SYNAL, H. A., SZIDAT, S., ZHANG, Y. L. 2013a. A versatile gas interface for routine radiocarbon analysis with a gas ion source. *Nuclear Instruments & Methods in Physics Research Section B-Beam Interactions with Materials and Atoms,* 294, 315-319.

WACKER, L., FUELOEP, R. H., HAJDAS, I., MOLNAR, M., RETHEMEYER, J. 2013b. A novel approach to process carbonate samples for radiocarbon measurements with helium carrier gas. *Nuclear Instruments & Methods in Physics Research Section B-Beam Interactions with Materials and Atoms,* 294, 214-217.

WANNER, C. 2007. Reduktion von Chromat mit Eisenpulver: Geologische Untersuchungen am Sanierungsfall Rivera, Laborversuche und geochemische Modellierungen. Masters thesis, University of Bern, Switzerland.

WIELAND, E., HUMMEL, W. 2015. Formation and stability of carbon-14 containing organic compounds in alkaline iron-water systems: Preliminary assessment based on a literature survey and thermodynamic modelling. *Mineralogical Magazine,* 79(6), 1275-1286.

WIELAND, E., TITS, J., ULRICH, A., BRADBURY, M. H. 2006. Experimental evidence for solubility limitation of the aqueous Ni(II) concentration and isotopic exchange of Ni-63 in cementitious systems. *Radiochimica Acta,* 94(1), 29-36.

YAMAGUCHI, T., TANUMA, S., YATSUTOMI, I., NAKAYAMA, T., TANABE, H., KATSURAI, K., KAWAMURA, W., MAEDA, K., KITAO, H. and SAIGUSA, M. 1999. A study on chemical forms and migration behaviour of radionuclides in hull wastes. *Radioactive*

Waste Managment and Environmental Remediation, *ICEM 99*, Sept 26-30, Nagoya, Japan, ASME.

YAMASHITA, Y., TANABE, H., SAKURAGI, T., TAKAHASHI, R., SASOH, M. 2014. C-14 release behavior and chemical species from irradiated hull waste under geological disposal conditions. *Materials Research Society Symposium Proceedings,* 1665, 187-194.

YIM, M.-S. and CARON, F. 2006. Life cycle and management of carbon-14 from nuclear power generation. *Progress in Nuclear Energy,* 48(1), 2-36.

7 Appendix

Table A 1: Summary of the results obtained by immersing pretreated Sigma-Aldrich powder in ACW I, ACW II and ACW III.

		Carboxylic acids [µM]			Hydrocarbons [µM]					
Solution	**Time [d]**	**Formate**	**Acetate**	**Oxalate**	**Methane**	**Ethane**	**Ethene**	**Propane**	**Propene**	**Butane**
ACW I	3E-04	n.d.	20 ± 5	1.7 ± 0.7	-	-	-	-	-	-
	1	n.d.	24 ± 2	4.9 ± 0.2	0.6 ± 0.1	n.d.	0.5 ± 0.1	n.d.	0.3 ± 0.1	n.d.
	2	n.d.	32 ± 6	7.9 ± 0.5	1.1 ± 0.2	0.2 ± 0.1	0.6 ± 0.1	n.d.	0.4 ± 0.1	n.d.
	7	9 ± 2	32 ± 6	10.4 ± 0.6	1.6 ± 0.2	0.3 ± 0.1	0.6 ± 0.1	0.2 ± 0.1	0.6 ± 0.1	0.1 ± 0.1
	14	6 ± 1	32 ± 4	11.7 ± 0.8	2.4 ± 0.3	0.4 ± 0.2	0.9 ± 0.1	0.4 ± 0.1	1.0 ± 0.1	0.2 ± 0.1
	21	6 ± 1	32 ± 5	10.4 ± 1.7	3.5 ± 0.5	0.7 ± 0.1	1.2 ± 0.2	0.6 ± 0.1	1.4 ± 0.2	0.3 ± 0.1
	28	7 ± 2	35 ± 6	10.0 ± 0.6	4.2 ± 0.7	0.9 ± 0.2	1.5 ± 0.2	0.8 ± 0.1	1.8 ± 0.2	0.5 ± 0.1
	35	8 ± 1	32 ± 5	9.2 ± 0.5	4.4 ± 0.9	0.9 ± 0.2	1.5 ± 0.3	0.8 ± 0.2	1.7 ± 0.4	0.4 ± 0.1
ACW II	3E-04	n.d.	22 ± 4	1.3 ± 0.3	-	-	-	-	-	-
	1	n.d.	n.d.	n.d.	0.6 ± 0.1	n.d.	0.4 ± 0.1	n.d.	0.3 ± 0.1	n.d.
	2	6 ± 3	41 ± 7	4.7 ± 0.6	1.3 ± 0.3	0.2 ± 0.1	0.6 ± 0.1	0.2 ± 0.1	0.4 ± 0.1	0.1 ± 0.1
	7	n.d.	n.d.	n.d.	1.2 ± 0.2	0.2 ± 0.1	0.5 ± 0.1	0.2 ± 0.1	0.5 ± 0.1	0.1 ± 0.1
	14	7 ± 1	31 ± 3	10.5 ± 1.5	1.2 ± 0.2	0.2 ± 0.1	0.6 ± 0.1	0.3 ± 0.1	0.5 ± 0.1	0.1 ± 0.1
	21	8 ± 2	29 ± 3	10.0 ± 1.8	1.3 ± 0.3	0.3 ± 0.1	0.8 ± 0.2	0.3 ± 0.1	0.6 ± 0.1	0.1 ± 0.1
	28	8 ± 3	32 ± 6	4.9 ± 0.2	1.1 ± 0.2	0.3 ± 0.1	0.7 ± 0.1	0.3 ± 0.1	0.6 ± 0.1	0.1 ± 0.1
	35	10 ± 5	39 ± 7	2.9 ± 1.9	1.3 ± 0.3	0.3 ± 0.1	0.7 ± 0.1	0.3 ± 0.1	0.5 ± 0.1	0.1 ± 0.1
ACW III	3E-04	-	-	-	-	-	-	-	-	-
	1	n.d.	n.d.	1.6 ± 0.3	1.5 ± 0.3	0.2 ± 0.1	0.6 ± 0.1	0.3 ± 0.1	0.5 ± 0.1	0.1 ± 0.1
	2	n.d.	n.d.	1.4 ± 0.2	1.8 ± 0.4	0.3 ± 0.1	0.7 ± 0.1	0.3 ± 0.1	0.6 ± 0.1	0.1 ± 0.1
	7	n.d.	n.d.	1.0 ± 0.1	1.9 ± 0.4	0.4 ± 0.1	0.7 ± 0.1	0.4 ± 0.1	0.6 ± 0.1	0.2 ± 0.1
	14	n.d.	n.d.	1.3 ± 0.1	1.8 ± 0.4	0.4 ± 0.1	0.8 ± 0.2	0.4 ± 0.2	0.7 ± 0.1	0.2 ± 0.1
	21	n.d.	n.d.	1.3 ± 0.2	1.9 ± 0.4	0.4 ± 0.1	0.9 ± 0.2	0.4 ± 0.2	0.8 ± 0.2	0.2 ± 0.1
	28	n.d.	n.d.	1.2 ± 0.2	1.7 ± 0.3	0.4 ± 0.1	0.9 ± 0.2	0.4 ± 0.1	0.8 ± 0.2	0.2 ± 0.1
	35	n.d.	n.d.	0.8 ± 0.1	1.3 ± 0.3	0.3 ± 0.1	0.8 ± 0.2	0.4 ± 0.1	0.7 ± 0.1	0.2 ± 0.1

n.d.: not determined meaning that the measurement is below LOD for the given compound (see Tables 6 - 8); not measured: -

Table A 2: Summary of the results obtained by immersing pretreated BASF powder in ACW I, ACW II and ACW III.

		Carboxylic acids [µM]			Hydrocarbons [µM]					
Solution	**Time [d]**	**Formate**	**Acetate**	**Oxalate**	**Methane**	**Ethane**	**Ethene**	**Propane**	**Propene**	**Butane**
ACW I	3E-04	n.d.	25 ± 3	1.2 ± 0.1	-	-	-	-	-	-
	1	12 ± 2	37 ± 5	1.5 ± 0.2	2.2 ± 0.6	0.6 ± 0.2	0.8 ± 0.2	0.4 ± 0.1	0.6 ± 0.1	0.1 ± 0.1
	2	11 ± 2	32 ± 6	1.5 ± 0.2	1.9 ± 0.4	0.4 ± 0.1	0.6 ± 0.2	0.2 ± 0.2	0.4 ± 0.1	0.1 ± 0.1
	7	12 ± 2	37 ± 6	1.4 ± 0.2	3.1 ± 0.6	0.7 ± 0.1	1.1 ± 0.2	0.6 ± 0.1	1.0 ± 0.2	0.2 ± 0.1
	14	12 ± 2	33 ± 6	0.3 ± 0.1	4.1 ± 0.8	1.0 ± 0.2	1.4 ± 0.3	0.8 ± 0.1	1.2 ± 0.2	0.3 ± 0.1
	21	12 ± 2	36 ± 5	0.5 ± 0.1	3.8 ± 0.8	1.2 ± 0.3	1.5 ± 0.3	1.0 ± 0.2	1.4 ± 0.3	0.4 ± 0.1
	28	11 ± 2	36 ± 6	0.2 ± 0.1	5.2 ± 1.0	1.4 ± 0.2	1.9 ± 0.4	1.1 ± 0.1	1.7 ± 0.3	0.4 ± 0.1
	35	12 ± 2	33 ± 6	0.1 ± 0.1	5.4 ± 1.1	1.5 ± 0.3	2.0 ± 0.4	1.2 ± 0.1	1.8 ± 0.4	0.5 ± 0.1
ACW II	3E-04	5 ± 2	26 ± 3	0.9 ± 0.2	-	-	-	-	-	-
	1	12 ± 3	35 ± 5	0.6 ± 0.1	2.2 ± 0.4	0.7 ± 0.1	0.8 ± 0.2	0.6 ± 0.1	0.6 ± 0.1	0.2 ± 0.1
	2	11 ± 3	35 ± 5	0.6 ± 0.1	2.1 ± 0.4	0.7 ± 0.1	0.7 ± 0.1	0.5 ± 0.1	0.5 ± 0.1	0.2 ± 0.1
	7	12 ± 2	37 ± 6	1.9 ± 0.3	2.0 ± 0.4	0.7 ± 0.2	0.8 ± 0.2	0.6 ± 0.2	0.6 ± 0.2	0.4 ± 0.1
	14	12 ± 2	38 ± 6	1.7 ± 0.2	2.3 ± 0.5	0.8 ± 0.1	0.8 ± 0.1	0.7 ± 0.1	0.6 ± 0.1	0.2 ± 0.2
	21	12 ± 3	37 ± 6	0.5 ± 0.1	2.1 ± 0.4	0.8 ± 0.2	0.8 ± 0.2	0.7 ± 0.2	0.7 ± 0.1	0.3 ± 0.1
	28	15 ± 3	40 ± 7	0.8 ± 0.1	1.9 ± 0.4	0.8 ± 0.1	0.7 ± 0.1	0.7 ± 0.1	0.7 ± 0.2	0.3 ± 0.1
	35	14 ± 3	37 ± 6	0.3 ± 0.1	1.9 ± 0.4	0.7 ± 0.2	0.7 ± 0.2	0.8 ± 0.2	0.6 ± 0.2	0.2 ± 0.2
ACW III	3E-04	-	-	-	-	-	-	-	-	-
	1	n.d.	n.d.	4.1 ± 0.2	7.6 ± 3.0	2.8 ± 1.2	1.8 ± 0.5	1.9 ± 0.7	1.5 ± 0.3	0.8 ± 0.2
	2	n.d.	n.d.	5.0 ± 0.2	4.3 ± 0.9	1.5 ± 0.2	1.3 ± 0.3	1.2 ± 0.1	1.0 ± 0.2	0.6 ± 0.1
	7	n.d.	n.d.	7.7 ± 0.4	4.6 ± 0.9	1.7 ± 0.2	1.4 ± 0.3	1.4 ± 0.2	1.2 ± 0.2	0.7 ± 0.1
	14	n.d.	n.d.	7.4 ± 0.4	5.5 ± 1.1	2.2 ± 0.3	1.7 ± 0.3	1.7 ± 0.3	1.4 ± 0.3	0.7 ± 0.1
	21	n.d.	n.d.	2.0 ± 0.1	5.1 ± 1.7	2.1 ± 0.9	1.5 ± 0.3	1.7 ± 0.5	1.4 ± 0.4	0.7 ± 0.3
	28	n.d.	n.d.	0.5 ± 0.1	3.5 ± 0.7	1.5 ± 0.3	1.3 ± 0.3	1.3 ± 0.3	1.1 ± 0.2	0.6 ± 0.1
	35	n.d.	n.d.	7.9 ± 0.4	2.0 ± 0.4	1.1 ± 0.3	1.2 ± 0.2	1.0 ± 0.5	1.1 ± 0.3	0.4 ± 0.3

n.d.: not determined meaning that the measurement is below LOD for the given compound (see Tables 6 - 8); not measured: -

Table A 3: Summary of the results obtained by immersing untreated Sigma-Aldrich powder in ACW I, ACW II and ACW III.

		Carboxylic acids [µM]			Hydrocarbons [µM]					
Solution	**Time [d]**	**Formate**	**Acetate**	**Oxalate**	**Methane**	**Ethane**	**Ethene**	**Propane**	**Propene**	**Butane**
ACW I	3E-04	-	-	-	-	-	-	-	-	-
	1	n.d.	n.d.	2.1 ± 0.1	0.8 ± 0.2	n.d.	0.4 ± 0.1	n.d.	0.3 ± 0.1	n.d.
	2	n.d.	n.d.	2.6 ± 0.1	1.0 ± 0.2	0.2 ± 0.1	0.5 ± 0.1	n.d.	0.4 ± 0.1	n.d.
	7	n.d.	n.d.	3.0 ± 0.1	2.5 ± 0.5	0.4 ± 0.1	1.5 ± 0.3	0.2 ± 0.1	1.2 ± 0.2	0.1 ± 0.1
	14	n.d.	n.d.	3.8 ± 0.2	3.1 ± 0.6	0.6 ± 0.2	1.6 ± 0.3	0.4 ± 0.1	1.4 ± 0.3	0.2 ± 0.1
	21	n.d.	n.d.	2.2 ± 0.1	2.9 ± 0.6	0.5 ± 0.2	1.6 ± 0.3	0.4 ± 0.1	1.5 ± 0.3	0.2 ± 0.1
	28	n.d.	n.d.	1.4 ± 0.1	1.2 ± 0.2	0.2 ± 0.1	0.6 ± 0.1	0.2 ± 0.1	0.6 ± 0.1	0.1 ± 0.1
	35	n.d.	n.d.	1.6 ± 0.1	1.2 ± 0.2	0.3 ± 0.1	0.6 ± 0.1	0.2 ± 0.1	0.6 ± 0.1	0.1 ± 0.1
ACW II	3E-04	-	-	-	-	-	-	-	-	-
	1	n.d.	n.d.	2.9 ± 0.1	0.9 ± 0.2	0.2 ± 0.1	0.4 ± 0.1	0.2 ± 0.1	0.3 ± 0.1	n.d.
	2	n.d.	n.d.	3.2 ± 0.2	1.1 ± 0.2	0.2 ± 0.1	0.5 ± 0.1	0.2 ± 0.1	0.4 ± 0.1	0.1 ± 0.1
	7	n.d.	n.d.	4.9 ± 0.2	1.1 ± 0.2	0.3 ± 0.1	0.5 ± 0.1	0.2 ± 0.1	0.4 ± 0.1	0.1 ± 0.1
	14	n.d.	n.d.	4.1 ± 0.2	0.9 ± 0.2	0.2 ± 0.1	0.5 ± 0.1	0.2 ± 0.1	0.4 ± 0.1	0.1 ± 0.1
	21	n.d.	n.d.	4.4 ± 0.2	1.0 ± 0.2	0.2 ± 0.1	0.5 ± 0.1	0.2 ± 0.1	0.4 ± 0.1	0.1 ± 0.1
	28	n.d.	n.d.	4.3 ± 0.2	1.0 ± 0.2	0.2 ± 0.1	0.4 ± 0.1	0.2 ± 0.1	0.4 ± 0.1	0.1 ± 0.1
	35	n.d.	n.d.	4.3 ± 0.2	1.1 ± 0.2	0.4 ± 0.1	0.5 ± 0.1	0.4 ± 0.1	0.5 ± 0.1	0.2 ± 0.1
ACW III	3E-04	-	-	-	-	-	-	-	-	-
	1	n.d.	n.d.	n.d.	2.0 ± 0.4	0.3 ± 0.1	0.7 ± 0.1	0.3 ± 0.1	0.6 ± 0.1	0.1 ± 0.1
	2	n.d.	n.d.	6.0 ± 0.3	3.1 ± 0.6	0.5 ± 0.1	1.1 ± 0.1	0.4 ± 0.1	0.9 ± 0.2	0.2 ± 0.1
	7	n.d.	n.d.	13.0 ± 0.6	4.6 ± 0.9	0.8 ± 0.2	1.5 ± 0.3	0.8 ± 0.2	1.4 ± 0.3	0.4 ± 0.1
	14	n.d.	n.d.	n.d.	4.8 ± 1.0	0.9 ± 0.2	1.6 ± 0.3	0.8 ± 0.2	1.6 ± 0.3	0.4 ± 0.1
	21	n.d.	n.d.	8.7 ± 0.4	4.5 ± 0.9	0.9 ± 0.2	1.6 ± 0.3	0.9 ± 0.2	1.8 ± 0.4	0.5 ± 0.1
	28	n.d.	n.d.	5.9 ± 0.3	4.0 ± 0.8	1.0 ± 0.2	1.9 ± 0.4	0.9 ± 0.2	2.1 ± 0.4	0.5 ± 0.1
	35	n.d.	n.d.	3.5 ± 0.2	6.3 ± 1.3	1.3 ± 0.3	3.1 ± 0.6	1.2 ± 0.2	4.1 ± 0.8	1.0 ± 0.2

n.d.: not determined meaning that the measurement is below LOD for the given compound (see Tables 6 - 8); not measured: -